The TITAN-II reversed-field-pinch fusion-power-core design

Clement P.C. Wong [a], Steven P. Grotz [b], Farrokh Najmabadi [b], James P. Blanchard [b,1],
Edward T. Cheng [a,2], Patrick I.H. Cooke [b,3], Richard L. Creedon [a,4], Nasr M. Ghoniem [b],
Paul J. Gierszewski [c], Mohammad Z. Hasan [b], Rodger C. Martin [b,5], Kenneth R. Schultz [a],
Shahram Sharafat [b], Don Steiner [d] and Dai-Kai Sze [e]

[a] *General Atomics, San Diego, CA 92186, USA*
[b] *Institute of Plasma and Fusion Research, University of California, Los Angeles, CA 90024-1597, USA*
[c] *Canadian Fusion Fuels Technology Project, Mississauga, Ontario, LSJ1K3, Canada*
[d] *Rensselaer Polytechnic Institute, Troy, NY 12180-3590, USA*
[e] *Argonne National Laboratory, 9700 S. Cass Ave., Argonne, IL 60439, USA*

TITAN-II is a compact, high-power-density reversed-field pinch fusion power reactor design based on the aqueous lithium solution fusion power core concept. The selected breeding and structural materials are $LiNO_3$ and 9-C low activation ferritic steel, respectively. TITAN-II is a viable alternative to the TITAN-I lithium self-cooled design for the reversed-field pinch reactor to operate at a neutron wall loading of 18 MW/m^2. Submerging the complete fusion power core and the primary loop in a large pool of cool water will minimize the probability of radioactivity release. Since the protection of the large pool integrity is the only requirement for the protection of the public, TITAN-II is a level 2 of passive safety assurance design.

1. Introduction

The TITAN research program is a multi-institutional [1] effort to determine the potential of the reversed-field-pinch (RFP) magnetic fusion concept as a compact, high-power-density, and "attractive" fusion energy system from economics (cost of electricity, COE), safety, environmental, and operational viewpoints.

In recent reactor studies, the compact reactor option [2–5] has been identified as one approach toward a more affordable and competitive fusion reactor. The main feature of a compact reactor is a fusion power core (FPC) with a mass power density in excess of 100 to 200 kWe/tonne. Mass power density (MPD) is

Present addresses:
1 University of Wisconsin, Fusion Technology Institute, Madison, WI 53706-1687, USA.
2 TSI Research, Solana Beach, CA 92075, USA.
3 On assignment from Culham Laboratory, Abington, Oxfordshire, UK.
4 Advanced Cryomagnetics, 7390 Trade Street, San Diego, CA 92121, USA.
5 Oak Ridge National Laboratory, Oak Ridge, TN 37831, USA.

defined [2] as the ratio of the net electric power to the mass of the FPC, which includes the plasma chamber, first wall, blanket, shield, magnets, and related structure. The increase in MPD is achieved by increasing the plasma power density and neutron wall loading, by reducing the size and mass of the FPC through decreasing the blanket and shield thicknesses and using resistive magnet coils, as well as by increasing the blanket energy multiplication. A compact reactor, therefore, strives toward a system with an FPC comparable in mass and volume to the heat sources of alternative fission power plants, with MPDs ranging from 500 to 1000 kWe/tonne and competitive cost of energy.

Other potential benefits for compact systems can be envisaged in addition to improved economics. The FPC cost in a compact reactor is a small portion of the plant cost and, therefore, the economics of the reactor will be less sensitive to changes in the unit cost of FPC components or the plasma performance. Moreover, since a high-MPD FPC is smaller and cheaper, a rapid development program at lower cost should be possible, changes in the FPC design will not introduce large cost penalties, and the economics of learning curves can be readily exploited throughout the plant life.

The RFP has inherent characteristics which allow it to operate at very high mass power densities. This potential is available because the main confining field in an RFP is the poloidal field, which is generated by the large toroidal current flowing in the plasma. This feature results in a low field at the external magnet coils, a high plasma beta, and a very high engineering beta (defined as the ratio of the plasma pressure to the square of the magnetic field strength at the coils) as compared to other confinement schemes. Furthermore, sufficiently low magnetic fields at the external coils permit the use of normal coils while joule losses remain a small fraction of the plant output. This option allows a thinner blanket and shield. In addition, the high current density in the plasma allows ohmic heating to ignition, eliminating the need for auxiliary heating equipment. Also, the RFP concept promises the possibility of efficient current-drive systems based on low-frequency oscillations of poloidal and toroidal fluxes and the theory of RFP relaxed states. The RFP confinement concept allows arbitrary aspect ratios, and the circular cross section of plasma eliminates the need for plasma shaping coils. Lastly, the higher plasma densities particularly at the edge, together with operation with a highly radiative RFP plasma, significantly reduce the divertor heat flux and erosion problems.

These inherent characteristics of the RFP [6] allow it to meet, and actually far exceed, the economic threshold MPD value of 100 kWe/tonne. As a result, the TITAN study also seeks to find potentially significant benefits and to illuminate main drawbacks of operating well above the MPD threshold of 100 kWe/tonne. The program, therefore, has chosen a minimum cost, high neutron wall loading of 18 MW/m^2 as the reference case in order to quantify the issue of engineering practicality of operating at high MPDs. The TITAN study has also put strong emphasis on safety and environmental features in order to determine if high-power-density reactors can be designed with a high level of safety assurance and with low-activation material to qualify for Class-C waste disposal.

An important potential benefit of operating at a very high MPD is that the small physical size and mass of a compact reactor permits the design to be made of only a few pieces and a single-piece maintenance approach will be feasible [7,8]. Single-piece maintenance refers to a procedure in which all of components that must be changed during the scheduled maintenance are replaced as a single unit, although the actual maintenance procedure may involve the movement, storage, and reinstallation of some other reactor components.

In TITAN designs, the entire reactor torus is replaced as a single unit during the annual scheduled maintenance. The single-piece maintenance procedure is expected to result in the shortest period of downtime during the scheduled maintenance period because: (1) the number of connects and disconnects needed to replace components will be minimized; and (2) the installation time is much shorter because the replaced components are pretested and aligned as a single unit before committment to service. Furthermore, recovery from unscheduled events will be more standard and rapid because complete components will be replaced and the reactor brought back on line. The repair work will then be performed outside the reactor vault.

To achieve the design objectives of the TITAN study, the program was divided into two phases, each roughly one year in length: the Scoping Phase and the Design Phase. The objectives of the Scoping Phase were to define the parameter space for a high-MPD RFP reactor and to explore a variety of approaches to major subsystems. The Design Phase focused on the conceptual engineering design of basic ideas developed during the Scoping Phase with direct input from the parametric systems analysis and with strong emphasis on safety, environmental, and operational (maintenance) issues.

Scoping Phase activities of the TITAN program were reported separately [1]. Four candidate TITAN FPCs were identified during the Scoping Phase:

(1) a self-cooled, lithium-loop design with a vanadium-alloy structure;

(2) an aqueous, self-cooled "loop-in-pool" design in which the entire FPC is submerged in a pool of water to achieve a high level of passive safety;

(3) a self-cooled FLiBe pool design using a vanadium-alloy structure; and

(4) a helium-cooled ceramic design with a solid breeder and silicon carbide structure.

Two of the above FPC designs were selected for detail evaluation during the Design Phase because of inadequate resources to pursue all four designs. The choice of which two concepts to pursue was difficult; all four concepts have attractive features. The lithium-loop design promises excellent thermal performance and is one of the main concepts being developed by the blanket technology program. The water-cooled design promises excellent safety features and uses more developed technologies. The helium-cooled ceramic design offers true inherent safety and excellent thermal performance. The molten-salt pool design is the only low-pressure blanket and promises a high degree of passive safety. The lithium-loop (TITAN-I) and the

aqueous "loop-in-pool" (TITAN-II) concepts were chosen for detailed conceptual design and evaluation in the Design Phase. The choice was based primarily on the capability to operate at high neutron wall load and high surface heat flux. The choice not to pursue the helium-ceramic and molten-salt designs should in no way denigrate these concepts. Both concepts offer high performance and attractive features when used at lower wall loads; these concepts should be pursued in future design studies.

The operating space of a compact RFP reactor has been examined using a comprehensive parametric systems model which includes the evolving state of knowledge of the physics of RFP confinement and embodies the TITAN-I and TITAN-II engineering approaches [9]. Two key figures of merit, the cost of electricity (COE) and mass power density (MPD), are monitored by the parametric systems model and are displayed in Figure 1 of the Introduction by F. Najmabi on p. 71 as functions of the neutron wall loading. This Figure shows that the COE is relatively insensitive to wall loadings in the range of 10 to 20 MW/m^2, with a shallow minimum at about 19 MW/m^2. The MPD is found to increase monotonically with the wall load. For designs with a neutron wall load larger than about 10

MW/m^2, the FPC is physically small enough such that single-piece FPC maintenance is feasible. These considerations point to a design window for compact RFP reactors with neutron wall loading in the range of 10 to 20 MW/m^2. The TITAN-class RFP reactors in this design window have an MPD in excess of 500 kWe/ tonne, and an FPC engineering power density in the range of 5 to 15 MWt/m^3; these values represent improvements by factors of 10 to 30 compared with earlier fusion reactor designs. The FPC cost is a smaller portion of the total plant cost (typically about 12%) compared with 25% to 30% for earlier RFP designs [4,5]. Therefore, the unit direct cost (UDC) is less sensitive to related physics and technology uncertainties.

Near-minimum-COE TITAN-I and TITAN-II design points, incorporating distinct blanket thermal-hydraulic options, materials choices, and neutronics performances have been identified in Figure 1 of the first article in this issues. The major parameters of the TITAN reactors are summarized in Table 1. In order to permit a comparison, the TITAN reference design points have similar plasma parameters and wall loadings allowing for certain plasma engineering analyses to be common between the two designs.

Table 1
Operating parameters of TITAN fusion power cores

	TITAN-I	TITAN-II
Major radius (m)	3.9	3.9
Minor plasma radius (m)	0.60	0.60
First wall radius (m)	0.66	0.66
Plasma current (MA)	17.8	17.8
Toroidal field on plasma surface (T)	0.36	0.36
Poloidal beta	0.23	0.23
Neutron wall load (MW/m^2)	18	18
Radiation heat flux on first wall (MW/m^2)	4.6	4.6
Primary coolant	Liquid lithium	Aqueous solution
Structural material	V–3Ti–1Si	Ferritic steel 9-C
Breeder material	Liquid lithium	$LiNO_3$
Neutron multiplier	none	Be
Coolant inlet temperature (°C)	320	298
First-wall-coolant exit temperature (°C)	440	330
Blanket-coolant exit temperature (°C)	700	330
Coolant pumping power (MW)	48	49
Fusion power (MW)	2301	2290
Total thermal power (MW)	2935	3027
Net electric power (MW)	970	900
Gross efficiency	44%	35%
Net efficiency	33%	30%
Mass power density, MPD (kWe/tonne)	757	806
Cost of electricity, COE (mill/kWh)	39.7	38.0

The TITAN RFP plasma operates at steady state using oscillating-field current-drive (OFCD) to maintain the 18 MA of plasma current. This scheme [10,11] utilizes the strong coupling, through the plasma relaxation process which maintains the RFP profiles [12], between the toroidal and poloidal fields and fluxes in
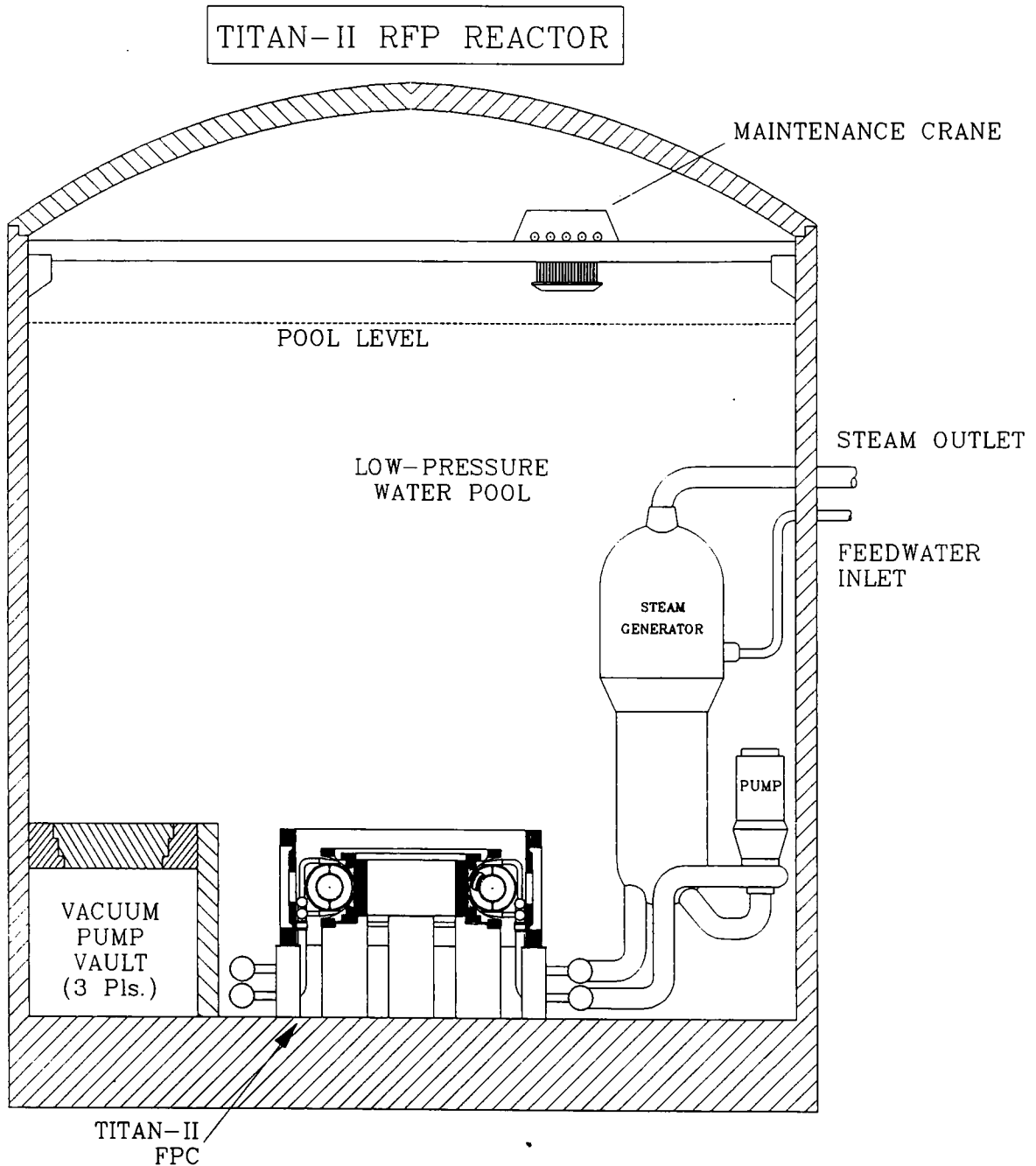

Fig. 1. Elevation view of the TITAN-II reactor building through the reactor centerline showing the water pool and the maintenance crane.

the RFP. Detailed plasma/circuit simulations have been performed which include the effects of eddy currents induced in the FPC. The calculated efficiency of the TITAN OFCD system is 0.3 A/W delivered to the power supply (0.8 A/W delivered to the plasma).

The impurity-control and particle-exhaust system consists of three high-recycling, toroidal-field divertors [13]. The TITAN designs take advantage of the beta-limited confinement observed in RFP experiments [14,15] to operate with a highly radiative core plasma, deliberately doped with a trace amount of high-Z Xe impurities [16]. The highly radiative plasma distributes the surface heat load uniformly on the first wall (4.6 MW/m^2). Simultaneously, the heat load on the divertor target plates is reduced to less than about 9 MW/m^2. The ratio of impurity density to electron density in the plasma is about 10^{-4}, Z_{eff} is about 1.7, and 70% of the core plasma energy is radiated (an additional 25% of the plasma energy is radiated in the edge plasma).

The "open" magnetic geometry of the divertors [17], together with the intensive radiative cooling, leads to a high-recycling divertor with high density and low temperature near the divertor target ($n_e \simeq 10^{21}$ m^{-3}, $T_e \simeq 5$ eV) relative to the upstream separatrix density and temperature ($n_e \simeq 2 \times 10^{20}$ m^{-3}, $T_e \simeq 200$ eV). The radial temperature profile is calculated to decay sharply to 2 eV near the first wall [16]. Negligible neutral-particle leakage from the divertor chamber to the core plasma and adequate particle exhaust are predicted. The first-wall and divertor-plate erosion rate is negligibly small because of the low plasma temperature and high density at that location.

2. Configuration

The elevation view of the FPC is shown in Fig. 1. Figures 4 and 5 of the Introduction on p. 74 in this issue show the general arrangement of the TITAN-II
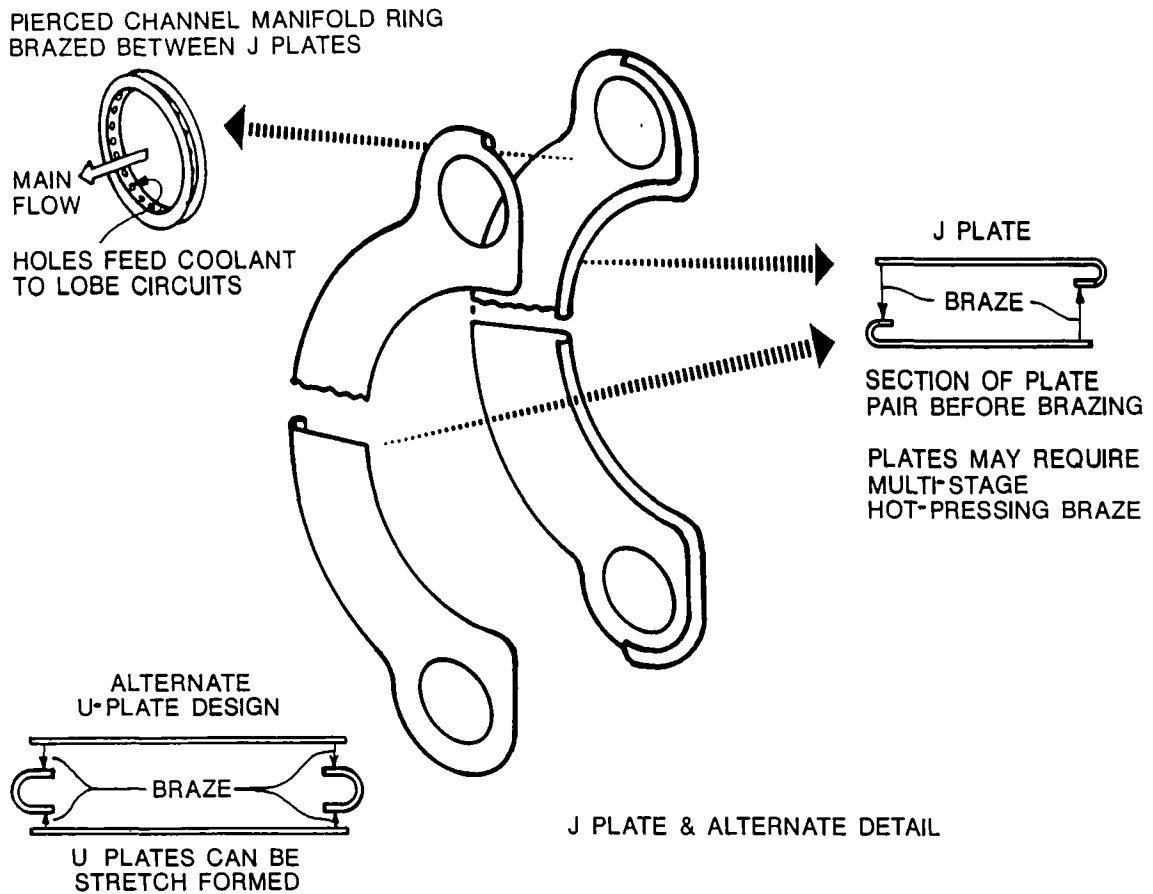

Fig. 2. The TITAN-II blanket lobe, J-plate design.

FIRST-WALL CHANNEL — BRAZED FRONT & REAR JOINT

2 SIMILAR PRESSINGS

CLAD NEUTRON MULTIPLIER RODS – 27.3-mm-O.D. TUBES 0.25-mm WALL CONTAINING 80% DENSE Be POWDER

HOT SHIELD CAST IN PIECES & WELDED TO FORM BLANKET CONTAINER

LOBE CONSTRUCTION

CERAMIC STANDOFF BUTTONS CLIPPED TO WATER-COOLED BLANKET SECTOR

DIVERTOR SHIELD

10 cm

30 cm

FIRST-WALL LINE

66 cm

CL

BLANKET RETAINER FRAMES PREVENT INNER LOBES FROM MOVING TOWARD TORUS CENTER
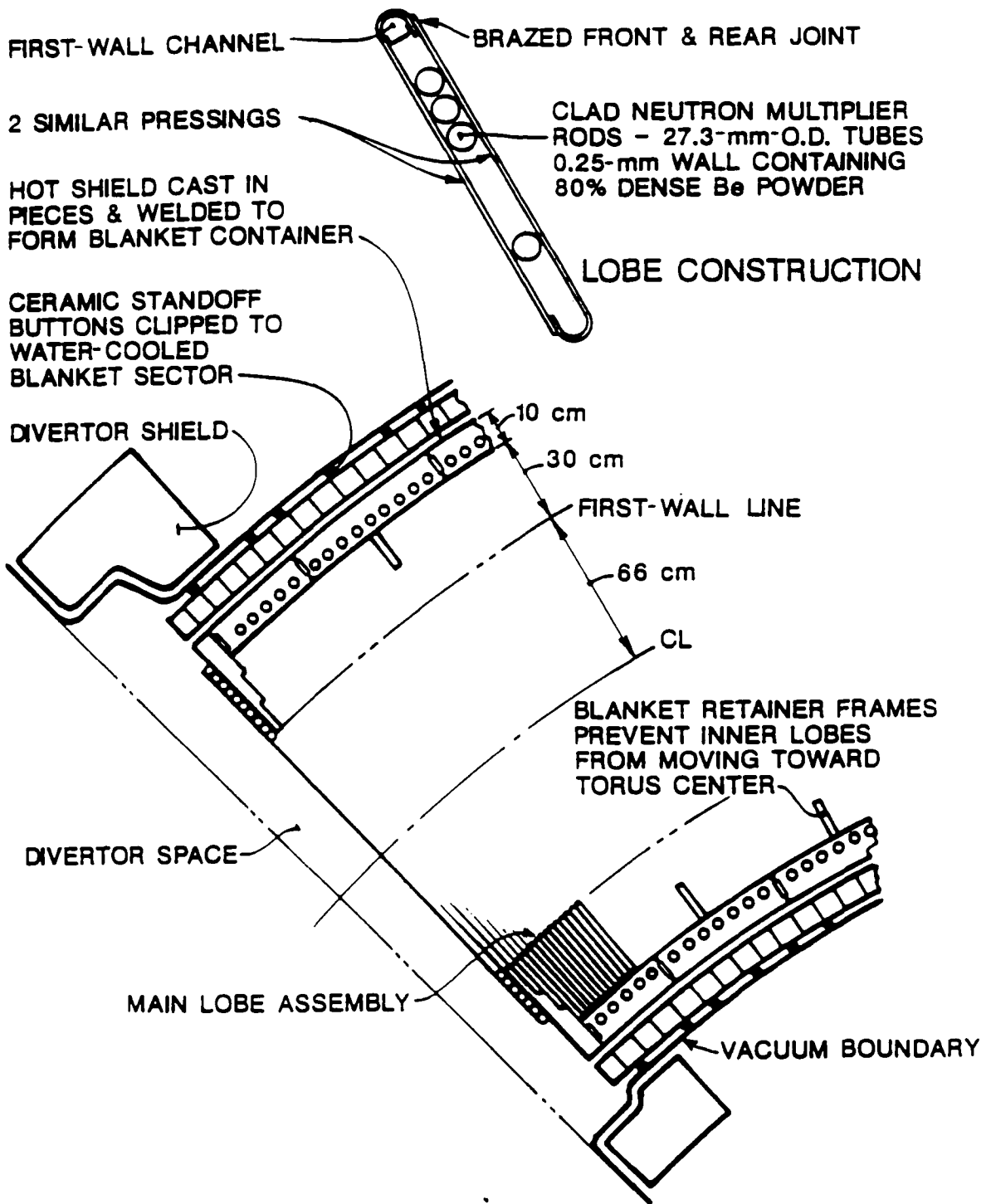
DIVERTOR SPACE

MAIN LOBE ASSEMBLY

VACUUM BOUNDARY

Fig. 3. Equatorial-plane cross section of a TITAN-II blanket module.

reactor. The major feature of the TITAN-II reactor is that the entire primary loop is located at the bottom of a low-temperature, atmospheric-pressure pool of pure water (Fig. 1). Detailed safety analyses were performed [18], which show that the TITAN-II pool can contain the afterheat energy of the FPC and will remain at a low enough temperature such that tritium or other radioactive material in the primary-coolant system will not be released.

The TITAN plasma is ohmically heated to ignition by using a set of normal-conducting ohmic-heating (OH) coils and a bipolar flux swing. The TITAN start-up requires minimum on-site energy storage, with the start-up power directly obtained from the power grid (maximum start-up power is 500 MW). The TITAN-II OH coils are cooled by pure water. A pair of relatively low-field superconducting equilibrium-field (EF) coils produce the necessary vertical field and a pair of small, copper EF trim coils provide the exact equilibrium during the start-up and OFCD cycles. The poloidal-field-coil arrangement allows access to the complete reactor torus by removing only the upper OH-coil set. The toroidal-field (TF) and divertor coils of TITAN-II are also composed of copper alloy.

The first wall and blanket of the TITAN-II design are integrated in the form of blanket lobes. The construction procedure for each blanket lobe is shown in Fig. 2. Each blanket lobe is made of two plates, called "J-plates" because one edge of each plate is rolled to the appropriate radius to form a J-section. Both J-plates are made of the low-activation, high-strength ferritic steel, 9-C [19]. The first-wall plate is thicker than the other plate, since it is subject to erosion. Two plates are then brazed or welded together to form a complete blanket lobe. A channel manifold ring completes the lobe and allows the coolant and breeder mixture to flow. This configuration will require a multistage pressing operation, perhaps even hot-pressing to achieve this shape.

An alternate design, also shown in Fig. 2, is the U-plate design. The advantages of this design are that the thin material can be used for both sides, and the edge U members are easier to make than the J-plates. However, acceptance of either configuration will depend on detailed investigation of the thick braze or weld area to ensure that there is no focusing of thermal radiation or other heat-transfer problems.

The outer dimensions of the blanket lobes are 3 cm toroidally and 30 cm radially. The lobe wall thickness is 1.4 mm. The cross section of the first wall is a semicircular channel with the convex side facing the plasma. The outer diameter is 3 cm, and the wall thickness of

1.5 mm includes a 0.25-mm allowance for erosion (the first-wall erosion is estimated to be negligible). A neutron multiplier zone is located behind the first wall and contains 7 rows of beryllium rods clad in 9-C alloy, with a diameter of 2.6 cm. The thickness of the clad is 0.25 mm. The multiplier zone is 20-cm long in the radial direction and contains 12% structure, 59% beryllium, and 29% coolant (all by volume). Nuclear heating rate in the blanket decreases away from the first wall, therefore, to ensure proper coolant velocity, poloidal flow separators are placed behind the 2nd, 4th, and 7th rows of beryllium rods to form channels which have individual orifices. The remaining 10 cm of the blanket lobe (the breeder/reflector zone) does not contain beryllium and consists of 9% structure and 91% coolant (by volume).

Seventy blanket lobes are then stacked side-by-side to form a blanket module. The structural details of a blanket module are shown in Fig. 3. This arrangement is structurally a membrane pressure vessel with balancing forces, derived from identical neighboring lobes, maintaining its flat sides. This configuration requires an external constraining structure to keep it pressed into oval form, which is readily derived from the shield as discussed below. The advantage of this design is that the structural fraction in the important near-first-wall radial zone is nearly as low as ideally possible, giving good tritium-breeding performance. This configuration also has a much lower void fraction when compared to a tubular design, giving a minimum-thickness blanket. The assembly technique for each blanket module is expected to be multistage brazing with intermediate leak checking. Since the lobes only require constraint in the blanket toroidal direction and because they are structurally soft in this direction, high precision is not necessary.

The TITAN-II FPC consists of three sectors, separated by the divertor modules. Four blanket modules are assembled together to form a sector. The shield is made of cast halfring sectors, welded together at the inside edge (Fig. 3) to form a blanket container. The shield is 10-cm thick in the radial direction and contains two rows of circular coolant channels. The volume percentages of structure and coolant in the shield are 90% and 10%, respectively.

The split at the top and bottom of the torus divides the blanket and the shield into inner and outer half shells which are structurally independent. The coolant channels are in the poloidal direction. The coolant enters at the bottom and exits at the top of the torus. One set of coolant channels runs along the out-board side of the torus and the other along the in-board side.

The tendency of the flat sides of a sector to blow out has to be resisted by what are, in effect, the divertor walls (Fig. 3). These walls are 12-cm-thick cantilever beam members which also derive some of their strength from their torsional stiffness and will require internal cooling. These walls are anchored to the shield shell by welds at the inside and outside of the shield.

Immediately behind the shield there is a 5-cm-thick zone occupied by the toroidal field (TF) coil which is a multi-turn copper coil held in position by ceramic standoffs from the shield (Fig. 3). The design of the TF-coil support elements is straightforward since the gravitational and magnetic forces on the TF coils are relatively small and are carried externally.

The vacuum boundary is a continuous, 5-mm-thick metal shell immediately outside the TF coil. Because of the large toroidal radius of 5.06 m, such a shell cannot withstand the atmospheric and water-pool pressures totaling about 3 atm without buckling. Accordingly, since the working stress is only about 7 MPa, nonconducting stabilizers similar to those used for the 5-cm-thick TF coil can be used. If necessary, the vacuum boundary can be electrically insulated in the toroidal direction by alternate layers of soft aluminum and hard, anodized 7075 aluminum-alloy sheets. The soft aluminum provides a deformable vacuum seal, and the anodized layer provides the electrical insulation. The two vacuum boundary skins can then be held together by 15-mm-thick stainless-steel, insulator-lined swagged clamps. Details of this method of vacuum-vessel insulation will still need to be demonstrated.

A number of electrically insulated penetrations of the vacuum shell also have to be made for the TF-coil leads. It is envisaged that the technology of automotive spark plugs can be developed to do this job. This consists of the embedment of a precision ceramic insulator in soft metal (usually copper) gaskets. This technique is presently available for diameters an order of magnitude larger than spark plugs, and its extension to sizes relevant to our task appears feasible. This also needs to be developed.

A skirt, welded to the lower header system and extended to the pool bottom, will support the entire removable first wall, blanket, and shield assembly. This skirt will be of open-frame form to allow free circulation of the pool.

The lifetime of the TITAN-II reactor torus (including the first wall, blanket, shield, and divertor modules) is estimated to be in the range of 15 to 18 MWy/m², with the more conservative value of 15 MWy/m² requiring the change-out of the reactor torus on a yearly basis for operation at 18 MW/m² of neutron wall loading at 76% availability. The TF coils are designed to last the entire plant life (30 full-power years). However, during the maintenance procedure, the TF coils are not separated from the reactor torus and are replaced each year. After the completion of the maintenance procedure, the used TF coils can be separated from the reactor torus and reused at a later time. The impact of discarding (not reusing) the TF-coil set annually is negligible on the COE.

3. Materials

The TITAN-II FPC is cooled by an aqueous lithium-salt solution which also acts as the breeder material [20]. Issues of corrosion and radiolysis, therefore, greatly impact the choice of the dissolved lithium salt and the structural material.

Two candidate lithium salts, lithium hydroxide (LiOH) and lithium nitrate ($LiNO_3$), are considered because they are highly soluble in water. The $LiNO_3$ salt is selected as the reference salt material for two main reasons. First, LiOH is more corrosive than $LiNO_3$ [21]. Recently, electrochemical corrosion tests were performed for LiOH and $LiNO_3$ aqueous solutions in contact with AISI 316 L stainless steels [22]. It was found that stainless steels, particularly low-carbon steels, exhibit better corrosion resistance in an $LiNO_3$ solution than in LiOH. From the point of view of radiolysis, lithium-nitrate solutions are also preferable. Radiolytic decomposition of water results in the formation of free radicals that will ultimately form highly corrosive hydrogen peroxide and OH ions. Nitrate ions (NO_3^-) in a lithium-nitrate solution, act as scavengers to reduce the probability of survival of highly reactive radicals in the water during exposure to radiation [21].

Among the candidate low-activation vanadium alloys, V–3Ti–1Si (the structural material for the TITAN-I design) had to be ruled out because of its poor water-corrosion resistance. Other vanadium alloys which contain chromium (e.g., V–15Cr–5Ti) show excellent resistance to corrosion by water coolant but their properties are inferior to those of ferritic steels when helium-embrittlement effects are taken into account [23]. Therefore, various steels were considered as TITAN-II structural material.

Reported results of the low-activation ferritic-steel (LAFS) development program indicate that a reduced-activation alloy can be developed without compromising mechanical properties, primarily by replacing Mo with W. For the TITAN-II reactor, the HEDL/UCLA 12Cr–0.3V–1W–6.5Mn alloy (alloy

9-C) has been chosen as the structural material primarily because of its high strength and good elongation behavior after irradiation as compared with other LAFSs [19]. The high chromium content of this alloy ensures an excellent corrosion resistance. The low carbon content of this alloy results in good weldability, high sensitization resistance [21], and reduces hydrogen-embrittlement susceptibility [21]. Furthermore, alloy 9-C has a low tungsten content (< 0.9%) which reduces the waste-disposal concerns of the production of the radionuclide ^{186m}Re by fusion-neutron reaction with W [24]. The high concentration of manganese in alloy 9-C prevents the formation of delta-ferrite phases, which is responsible for high ductile-to-brittle transition temperature (DBTT) and low hardness. The composition (wt%) of alloy 9-C was determined by the vendor as: 11.81Cr, 0.097C, 0.28V, 0.89W, 6.47Mn, 0.11Si, 0.003N, < 0.005P, 0.0055 with the balance in iron.

Radiolytic decomposition of aqueous solutions exposed to a radiation environment is always cause for concern. Radiolysis of pure water and of aqueous $LiNO_3$ salt solutions by light particles (e, γ, X ray) and heavy particles (n, p, T, α) was investigated. Gamma-ray radiolysis yields of $LiNO_3$ salt solutions are known as a function of salt concentration. At high concentrations, the H_2 yields are very small and the H_2O_2 yield decreases by a factor of about 3 relative to pure water. Oxygen yields of light-particle radiation are fairly independent of the salt concentration.

Energetic alpha particles (~ 2 MeV) are produced by nuclear reactions with lithium in the aqueous $LiNO_3$ salt solution. Reaction yields were estimated as a function of salt concentration based on the power law measurements of 3.4 MeV alpha particles. The oxygen production by heavy-particle radiation increases while the yields of H_2, H_2O_2, H, OH, and HO_2 all decrease with increasing salt concentration. The increase in oxygen production due to radiolysis may be balanced by the production of tritium atoms. It has been shown that oxygen added to non-boiling fission-reactor coolants at high power levels rapidly combines with any hydrogen present. The decrease in the yield of free radicals in concentrated $LiNO_3$ solutions makes this salt more favored than LiOH solutions.

The effect of elevated temperature on radiolysis was investigated. From experience gained in the fission industry with pure water, it can be ascertained that the stability of non-boiling water to radiolysis increases as temperature increases. The apparent stability is actually caused by an increase in recombination-reaction rates of radicals at elevated temperatures.

In summary, although many uncertainties remain and much research is required in the area of radiolysis, the use of a highly concentrated, aqueous $LiNO_3$ salt solutions should not lead to the formation of volatile or explosive gas mixtures. The effects of radiolytic decomposition products on corrosion, however, remain uncertain and experimental data on the behavior of radiolytic decomposition products in a fusion environment are needed.

Stress-corrosion cracking (SCC) is a major concern in the nuclear industry. Most recent experiences with SCC in a nuclear environment clearly show that reducing the oxygen content through the addition of hydrogen to the coolant can reduce SCC in most ferritic and austenitic alloys. The production of tritium in an aqueous lithium-salt solution is seen as an SCC controlling mechanism. The proper choice of structural material can further reduce the probability of SCC. In particular, a high chromium content together with a low carbon content is shown to reduce SCC. The ferritic alloy, 9-C, fulfills this requirement.

Experience with various aqueous nitrate-salt solutions shows that the choice of the cation will affect the degree of corrosion attack. The aggressiveness of nitrates decreases with choice of cation in the following order: NH_4, Ca, Li, K, and Na. Thus, for the $LiNO_3$ salt, the aggressiveness of NO_3^- ions is in the medium range. The effect of the cation choice on SCC has been related to the acidity of the solution. Investigations into buffering the $LiNO_3$ salt solutions to an optimum pH value could lead to a marked reduction in the aggressiveness of the solution. Reduction of the oxidizing strength of the salt solution has been found to retard failure of test samples by SCC. On the other hand, an increase in the oxidizing power of the solution decreases radiolytic decomposition rates. An optimum oxidizing strength will have to be established experimentally since the number of factors involved are too large to make analytical predictions.

Recent experiments [25] on the corrosion rates of $LiNO_3$ salt solutions with 316 SS and a martensitic alloy at 95 and 250°C show a lack of a marked transition between the primary and secondary passive regions. This data implies that a relatively stable passive layer is formed in this salt. Microscopic examination of the 316 SS showed that a smooth oxide film was formed on the metal surface in $LiNO_3$, with the roughness independent of solution concentration and temperature. Recently, electrochemical corrosion tests were performed for aqueous LiOH and $LiNO_3$ solutions in contact with AISI 316 L stainless steel [22]. It was found that stainless steels, particularly low-carbon

steels, exhibit better corrosion resistance in $LiNO_3$ solution than in LiOH.

It should be noted that most of the above experimental findings regarding corrosion and SCC of steels in $LiNO_3$ salt solutions were obtained without any control of the oxygen content of the solution which plays a significant role in corrosion processes. In a fusion environment, the production of tritium will undoubtedly affect the oxygen content of the aqueous solution through recombination. Thus, breeding of tritium in the aqueous solution can potentially reduce corrosion and SCC of the structural material used in the FPC.

The investigation of the corrosion of ferritic steels in an aqueous $LiNO_3$ salt solution does not show unexpectedly high corrosion rates or high susceptibility to SCC. In addition, the latest experimental findings do not indicate any unforeseen catastrophic corrosion attack. However, an extensive research effort needs to be undertaken to confirm these observations. Furthermore, the effects of high-energy neutron irradiation on corrosion mechanisms and rates should be examined.

Another form of attack on structural material in an aqueous environment is hydrogen embrittlement, caused primarily by the trapping of absorbed hydrogen in metals under applied stresses. The main factor influencing hydrogen embrittlement is the hydrogen content, which depends strongly on the temperature, microstructure, and strength of the alloy. Hydrogen content can be reduced by minimizing the source of nascent hydrogen (mostly due to corrosion) and by operating at high temperatures ($> 200°C$), provided that a low-carbon steel is used. High concentrations of chromium, nickel, or molybdenum (> 10 wt%) increase the resistance of ferrous alloys to hydrogen damage. Microstructural features (e.g., a fine-grained and annealed alloy with minimum cold work) further reduce susceptibility to hydrogen embrittlement. Because of the lower strength and higher ductility of ferritic steels, these alloys are generally less susceptible to hydrogen embrittlement than austenitic steels.

Atomic hydrogen is produced on metal surfaces during corrosion processes. Thus, minimizing corrosion also reduces hydrogen embrittlement of the structure. The addition of nitrate salts to the aqueous solution reduces the corrosion rate of ferrous alloys [21], resulting in a reduction in the production of hydrogen atoms on the surfaces, and thus reducing the nascent hydrogen content. The production of tritium in the coolant does not necessarily result in an increased hydrogen attack because of rapid recombination to form molecular hydrogen or water molecules. The production of

hydrogen by nuclear reactions and by plasma-driven permeation through the first wall of a fusion device increases the hydrogen content inside the alloy matrix which may lead to unacceptable hydrogen embrittlement of the structure for operation at or near room temperature (the highest susceptibility of high-strength alloys to hydrogen embrittlement is at or near room temperature [26]). But the TITAN-II structural material operates at high temperatures ($> 400°C$), minimizing the effective trapping of hydrogen inside the matrix. Experiments show that above $\sim 200°C$, hydrogen embrittlement of ferrous alloys is reduced markedly [27]. Furthermore, the Nelson curves [28], used by the petrochemical industry as guidelines, show that chromium steels can operate at 400°C with a hydrogen partial pressure of 17 MPa without experiencing internal decarburization and hydrogen embrittlement [26].

Based on the above discussion, the ferritic alloy 9-C is expected to exhibit a high resistance to hydrogen embrittlement. The number of factors influencing hydrogen embrittlement are numerous and their interdependence is a complex function of the specific microstructure and operating conditions of an alloy. Therefore, experimental data are needed in order to perform a complete evaluation of hydrogen embrittlement of the 9-C alloy under TITAN-II operating conditions.

The physical properties of concentrated solutions of $LiNO_3$ at high temperatures differ from those of pure water. Therefore, the exact coolant conditions should be considered in designing the blanket. The thermal-hydraulic design of an aqueous-salt blanket can be very different from that of a water-cooled design, and advantage can be taken of the differences in properties by, for example, reducing the coolant pressure or increasing the temperature without incurring an increased risk of burnout.

A fairly detailed investigation of the physical properties of the aqueous solutions was made, including an extensive literature survey, to ensure that reliable data were used in analyzing the performance of the TITAN-II FPC. In many cases, experimental data for some physical properties of interest for $LiNO_3$ solutions are not available at high temperatures. Where this is the case, and reasonable extrapolations cannot be made, the corresponding data for NaCl solutions have been used. The $NaCl-H_2O$ system has been much more widely studied than any other solution and many solutions of 1-1 electrolytes (e.g., NaCl, KBr, and $LiNO_3$) have similar properties at the same concentrations. It is expected that such estimates should be accurate to about 20% [29], which is adequate for a worthwhile
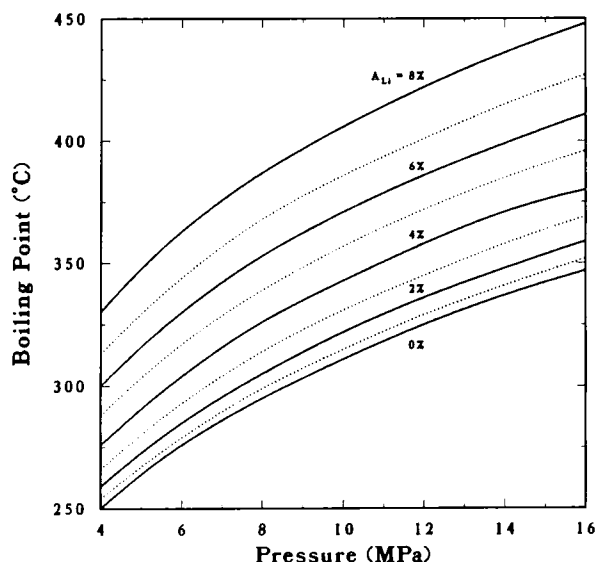
Boiling Point of LiNO₃ Solution

Fig. 4. Boiling temperatures of LiNO₃ solutions at various pressures and for a range of lithium-atom percentages (A$_{Li}$).

assessment of the thermal performance of the blanket to be made.

The physical properties of LiNO₃ solutions as a function of temperature and salt concentration are given in Section 10.2.3. The most drastic effect of adding LiNO₃ to the coolant water lies in the elevation of the boiling point of the solution. This implies that the thermal-hydraulic design of such an aqueous-salt blanket will be different from that of a pure-water-cooled design. Therefore, a lower coolant pressure or a higher operating temperature can be chosen. The estimated boiling temperature of the LiNO₃ solutions at various pressures are shown in Fig. 4 for a range of lithium-atom concentration in the aqueous coolant.

Many of the estimates of the properties of LiNO₃ aqueous solution are extrapolations from experimental data or have been obtained from the results for other salt solutions. Although these predictions should give good indications of the expected trends for the various properties, a much expanded experimental data base is required for the salts and conditions proposed before the thermal performance of an aqueous-salt blanket at high temperature can be confidently predicted.

The TITAN-II design requires a neutron multiplier to achieve an adequate tritium-breeding ratio. Beryl-

lium is the primary neutron multiplier for the TITAN-II design. Corrosion of beryllium in aqueous solutions is a function of the cleanliness of the beryllium surface and of solution impurities. Beryllium surfaces should be free of carbonates and sulfates and the water should have minimum chlorate and sulfate impurities to assure minimum corrosion rates. Coatings to protect beryllium against attack have been developed and their effectiveness has been demonstrated in a neutron-free environment. Research is needed to develop coatings that can withstand harsh radiation environments. For the TITAN-II design, a cladding of 9-C surrounds the beryllium rods.

Swelling levels of above ~ 10% will most likely result in a network of interlinking helium bubbles, thus promoting helium release. This means that swelling will stop temporarily until large enough temperature gradients cause sintering of open channels. The sintering temperature for beryllium has been estimated to be around 660°C. The ongoing process of closing and opening of porosity will ultimately lead to an equilibrium helium-venting rate with an associated maximum swelling value. Realistic prediction of this process is currently not feasible because of the lack of experimental data. A phenomenological swelling equation for beryllium is developed which predicts a maximum swelling value between 9% and 15% depending on the amount of retained helium atoms. A swelling value of 10% is taken as the basis for design calculations. Swelling may be accommodated, to a degree, by employing beryllium with low theoretical density (N 70%). This density can easily be achieved by using sphere-packed beryllium. The maximum operating temperature must be kept below 660°C to prevent sintering of the spheres.

Two methods for accommodating the high rate of swelling in beryllium are available: (1) using a very fine grain beryllium operating at temperatures above 750°C to ensure interlinkage of bubbles to vent the helium gas into the plenum of the cladding tube and (2) using sphere-packed beryllium with a low theoretical density (about 70%) and accumulating the helium inside the porosity. The latter approach, however, results in a lower neutron multiplication and a reduction of thermal conductivity.

Irradiation data on the strength of beryllium are sparse. Irradiation hardening does occur at temperatures above 300°C. McCarville et al. [30], predict that thermal creep may help extend the lifetime by relieving stresses caused by differential swelling, with irradiation-creep effects being negligible.

4. Neutronics

Neutronics calculations for the TITAN-II design were performed with ANISN [31], a 1-D neutron and gamma-ray transport code, using a P_3S_8 approximation in cylindrical geometry. The nuclear data library ENDF/B-V-based MATXS5 was used. The energy group structures in this library are 30 groups for the neutron cross sections and 12 groups for the gamma-ray cross sections. The library was processed with the NJOY system at Los Alamos National Laboratory [32] for coupled neutron and gamma-ray transport calculations. Neutronics scoping studies are performed with the configurational parameters based on the coupled mechanical and thermal-hydraulic design evaluations of the TITAN-II FPC.

Scoping calculations were performed for several combinations of blanket and shield thicknesses and different levels of ^{6}Li enrichment in the $LiNO_3$ salt dissolved in the water coolant. The option of using heavy water (D_2O) as the coolant for TITAN-II design was also considered, since D_2O has a lower neutron absorption cross section compared to ordinary water (H_2O). It is of interest to determine if heavy water can be used alone without any beryllium for the TITAN-II design. The effects of the beryllium density factor on the neutronics performance of the TITAN-II design were also studied. It is found that:

(1) The thickness of the Be zone or the level of ^{6}Li enrichment can be adjusted to obtain the desired tritium-breeding ratio (TBR). A 0.15-m-thick Be zone with 30% ^{6}Li enrichment level results in a TBR of 1.2.

(2) The ordinary-water blanket has a higher TBR than the one cooled by heavy water, within the range of blanket parameters used. The reason is that hydrogen has a better neutron moderation capability then deuterium. As a result, the neutron leakage into the TF coils is also higher for heavy-water blanket.

(3) Without beryllium, both H_2O and D_2O aqueous nitrate-salt blankets have insufficient TBR. Marginal TBR can be achieved for a heavy-water blanket if the structural content is reduced to 1% to 2%.

(4) For blankets that were considered, the blanket-energy multiplication ranges from 1.25 to 1.4.

Based on the neutronics scoping studies, the reference design of the TITAN-II reactor was determined and is illustrated in Fig. 5. The neutronics performance of the reference design is given in Table 2. The ^{6}Li enrichment level is 12%, beryllium density factor is 0.9, TBR is 1.2, and the blanket-energy multiplication is
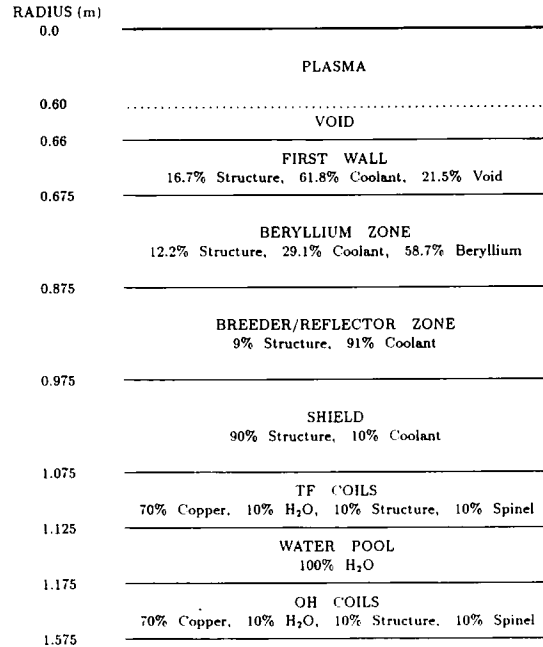
RADIUS (m)

Fig. 5. Schematic of the blanket and shield for the TITAN-II reference design. The coolant is an aqueous lithium-nitrate salt solution (6.4 at.% Li) and beryllium is 90% dense.

1.36. The fast-neutron flux at the TF coils is about 3×10^{25} n/m^2 and the total fast-neutron fluence on the TF coils after 30 full-power years of operation is about 1×10^{27} n/m^2, about a factor of 2 to 3 below the lifetime estimate for the spinel insulator.

Table 2
Neutronics performance of the TITAN-II reference design

Beryllium zone thickness (m)	0.2
Breeder/reflector zone thickness (m)	0.1
Shield thickness (m)	0.1
^{6}Li enrichment (%)	12.0
Tritium-breeding ratio	1.22
Blanket-energy multiplication, M	1.36
Fraction (% of M) of nuclear energy in	
First wall	12.4
Beryllium zone	69.2
Breeder/reflector zone	12.7
Shield	5.7
Energy leakage (% of M) to	
TF coils	1.27
Water pool	0.31
OH coils	1.09
TOTAL:	2.67

5. Thermal and structural design

The TITAN-II design uses an aqueous salt solution as the coolant. The coolant circulation is essentially loop-type, similar to that of TITAN-I, although the geometry of the blanket-coolant channels is very different. The salt is $LiNO_3$ and its lithium atom concentration is 6.4 at% with a ^6Li enrichment of 12%. The aqueous salt solution has two advantages as coolant. First, the coolant can act as tritium breeder. Second, the salt content elevates the boiling point of the coolant which can be utilized to reduce primary-coolant pressure below the pressure in the steam generator, eliminating the need for intermediate heat exchangers. Pressure reduction in a pure-water system cannot be realized because of the lower saturation temperature and the resulting lower critical heat flux.

The design peak heat flux on the TITAN-II first wall is 4.6 MW/m^2, corresponding to a plasma radiation fraction of 0.95. The inlet and exit temperatures of the coolant are, respectively, 298 and 330°C. The resulting exit subcooling is 17°C and, at moderate coolant velocities, nucleate boiling will take place in the first-wall coolant channels because of the high heat flux. Therefore, the mode of heat transfer in the first-wall coolant channels will be subcooled flow boiling (SFB).

In any application of boiling heat transfer, it must be ensured that the maximum possible heat flux is less than the critical heat-flux (CHF) limit by a certain safety margin. A large amount of data for CHF of pure liquids, especially for water, is available and numerous empirical correlations for the CHF exist. Because of the scatter in the data, these correlations are generally accurate to $\pm 20\%$ over the applicable range of the data [33]. In the absence of any CHF correlations specifically for high-temperature aqueous solutions, a general correlation, derived for water, has been used. This correlation for CHF, q''_{CHF}, was developed by Jens and Lottes [34] and has the range of parameters for boiling heat transfer which is close to those of the first-wall coolant channel of TITAN-II. Conversion to more convenient units of MW/m^2 yields

$$q''_{CHF} = C \left(\frac{G}{1356} \right)^m (\Delta T_{sub})^{0.22}, \qquad (1)$$

where G is the mass velocity of the coolant $(= \rho v)$ in kg/m^2s, the factor 1356 aries from the conversion of units, and ΔT_{sub} is the local subcooling in °C. Constants C and m depend on the pressure, p, through:

$$C = 3.00 - 0.102 p, \qquad (2)$$

$$m = p/30 + 0.04. \qquad (3)$$

Data used in deriving the above CHF correlation was limited to maximum values of critical heat flux of 38 MW/m^2, water velocity of 17 m/s, pressure of 13.6 MPa, and local subcooling of 90°C.

Because of the scatter in the data for critical heat flux, the maximum heat flux on the TITAN-II first wall is kept within 60% of that predicted by the correlation of Jens and Lottes so that an adequate safety margin for CHF is available. References cited in [33] show that the CHF is increased by about 40% in an aqueous solution of ethanol compared with that of pure water. Since CHF correlation for pure water is used for TITAN-II design, any increase in the CHF because of the lithium salt content will add to the safety margin.

The important temperatures in the blanket and shield are those at the center of the beryllium rods, the clad, the channel wall, and the maximum temperature in the shield region which should not exceed the design limits. In the blanket and shield regions, the heat flux removed by the coolant is very low, and the coolant flow is turbulent. Forced-convective heat transfer is adequate to remove the heat without raising the wall temperature to the level which would initiate nucleate boiling. Therefore, the maximum structure temperatures in the blanket and shield are calculated under the condition of non-boiling, forced-convective heat transfer.

The thermal-hydraulic design for TITAN-II FPC is found based on certain constraints such as the maximum allowable structure temperature (550°C), maximum allowable pressure and thermal stresses in the structure (respectively, 200 and 400 MPa), coolant velocities, and pumping power. The inlet and exit temperatures of the primary coolant are set, respectively, at 298 and 330°C in order to use an existing fission pressurized-water-reactor-type (PWR) power cycle. Because the salt content elevates the boiling point of the coolant, the primary-coolant pressure is reduced to 7 MPa, below the pressure in the steam generator, thus eliminating the need for intermediate heat exchangers. The thermal-hydraulic reference design of TITAN-II first wall is given in Table 3.

The thermal-hydraulic design of TITAN-II is expected to have adequate safety margins. The maximum heat flux crossing the coolant film in the first-wall channel is 5.1 MW/m^2, 63% lower than the critical heat flux (8.34 MW/m^2). The maximum temperature at the mid-plane of the first wall is 503°C which is less than the allowable limit of 550°C. The structure temperatures in the blanket and shield coolant channels have even greater safety margins. The maximum pressure stress is less than 50% of the allowable, and the thermal stress is below its limit.

Among other effects of the salt content, the specific heat capacity is reduced by a factor of about two while the density increases only by 15% which results in a significant reduction in the heat capacity of the coolant. The temperature rise of the primary coolant is 32°C. Therefore, although the coolant pressure drop is only 1 MPa, the large coolant-volume flow rate (39 m3/s) results in a pumping power of 49 MW, which is very

close to that for TITAN-I. For coolant circulation, pumps supplying a head of 1 MPa are used. Because the coolant flows in parallel through the first wall, multiplier, reflector, and shield zones, orifices are used to reduce the pressure as necessary for each channel. Separate coolant supplies for each of the flow channels (or zones) would alleviate the need for orifices and reduce the pumping power considerably. However, the
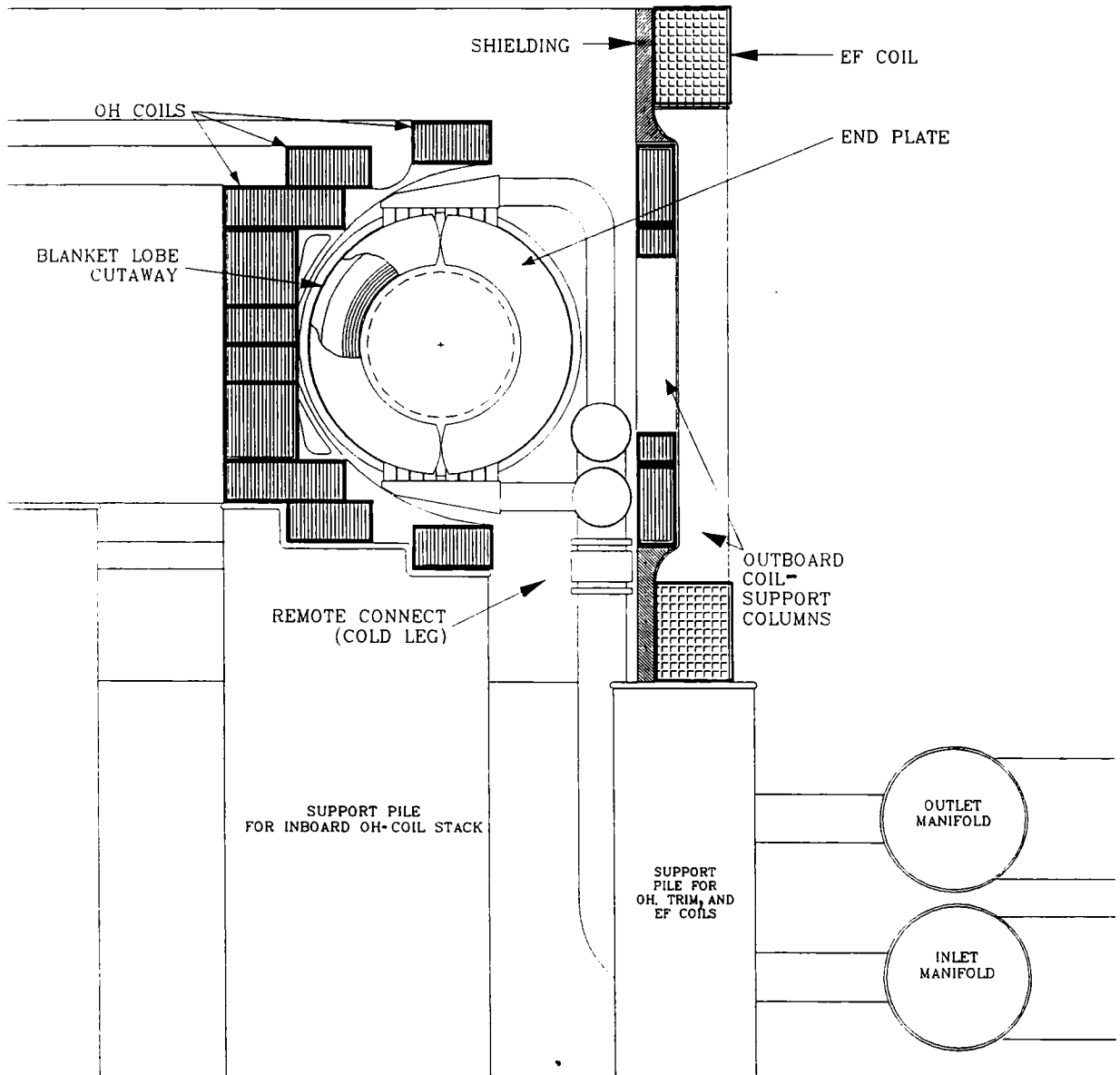
Fig. 6. Poloidal cross section of the TITAN-II fusion power core.

added complexity of more coolant systems and hydraulic separation of the flow channels does not justify this change.

6. Magnet engineering

Two types of magnets are used in the TITAN-II design (Fig. 6). The ohmic-heating (OH), equilibrium-field (EF) trim, divertor coils, and toroidal-field (TF) coils are normal-conducting with copper alloy as the conductor, spinel as the insulator, and pure water as the coolant. The main EF coils are made of NbTi superconductor and steel structural material. The poloidal-field coils are designed to last the life of the plant. The TF coils are removed with the FPC during the scheduled maintenance but are reused on a new torus afterwards. Because of the simple geometry of the TITAN-II magnets, the robust support structure, and the relatively low field produced by these coils, little or no extrapolation of current technology should be required.

Table 3
thermal-hydraulic design of TITAN-II first wall

Channel outer diameter, b	30.0 mm
Channel inner diameter, a	27.0 mm
Wall thickness, t	1.5 mm
Erosion allowance	0.25 mm
Structure volume fraction	0.17
Coolant volume fraction	0.62
Void volume fraction	0.21
Volumetric heating (structure)	202 MW/m^3
Volumetric heating (coolant)	270 MW/m^3
Total thermal power	770.2 MW
Coolant inlet temperature, T_{in}	298°C
Coolant exit temperature, T_{ex}	330°C
Maximum wall temperature, $T_{w,max}$	503°C
Coolant pressure, p	7 MPa
Maximum primary stress	98 MPa
Maximum secondary stress	363 MPa
Coolant flow velocity, U	22.6 m/s
Mass flow rate	1.15×10^4 kg/s
Volumetric flow rate	10 m^3/s
Pressure drop, Δp	0.5 MPa
Total pumping power	12.5 MW
Reynolds number, Re	1.49×10^6
Nusselt number, Nu	2360
Prandtl number, Pr	16.5
Critical heat flux, q''_{CHF}	8.3 Mw/m^2
Subcooling at exit, $T_{ex,sub}$	17°C

Table 4
TITAN-II reference power cycle

Primary coolant (water)	
Total thermal power	3027 MW
Inlet temperature	298°C
Exit temperature	330°C
Coolant pressure	7 MPa
Saturation temperature	347°C
Exit subcooling	17°C
Mass flow rate	4.5×10^4 kg/s
Total pumping power	49 MW
Throttle steam conditions	
Temperature	308°C
Pressure	7.2 MPa
Saturation temperature	289°C
Degree of superheat	19°C
Gross thermal efficiency	0.35

7. Power cycle

The selection of the inlet and exit temperatures of the TITAN-II primary coolant (respectively, 298 and 330°C) is motivated by the possibility of using an existing PWR-type power cycle. The lithium-salt content of the aqueous coolant (6.4 at%) elevates the boiling point of the coolant from 285°C for pure water to 347°C at a pressure of 7 MPa. Since the primary-coolant pressure is less than the steam pressure in the steam generator (7.2 MPa), any leakage in steam generator tubes will not result in the primary coolant leaking into the steam side. Therefore, the TITAN-II reference design uses a power cycle without an intermediate heat exchanger, which results in an increase in the power cycle efficiency. The parameters of TITAN-II reference power cycle are given in Table 4. The steam cycle conditions are similar to those of existing PWR-type power cycles [35]. The estimated gross thermal efficiency of the TITAN-II power cycle is 35%.

8. Divertor engineering

The design of the impurity-control system poses some of the most severe problems of any component of a DT fusion reactor. The final TITAN-II divertor design represents the result of extensive iterations between edge-plasma analysis, magnetic design, thermal-hydraulic and structural analyses, and neutronics.

The TITAN-II impurity-control system is based on the use of toroidal-field divertors to minimize the perturbation to the global magnetic configuration and to

minimize the coil currents and stresses. The TITAN divertor uses an "open" configuration, in which the divertor target is located close to the null point, facing the plasma, rather than in a separate chamber. This positioning takes advantage of the increased separation between the magnetic-field lines (flux expansion) in this region, which tends to reduce the heat loading on the divertor plate because the plasma flowing to the target is "tied" to the field lines. The high plasma density in front of the divertor target ensures that the neutral particles emitted from the surface have a short mean free path; a negligible fraction of these neutral particles enter the core plasma [13].

The TF-coil design for TITAN-II, which consists of copper coils as opposed to the integrated-blanket coils (IBC) of TITAN-I, prompted a new divertor magnetic design. The final magnetic design, similar to that of TITAN-I, includes three divertor modules which are located 120° apart in the toroidal direction. An equatorial-plane cross section of the one of the divertor modules is shown in Fig. 7. The magnetic-field lines are diverted onto the divertor plate using one nulling and two flanking coils with the latter localizing the nulling effect (divertor-trim coils are not required as opposed to the the TITAN-I design). The TITAN-II divertor coils are made of copper and the joule losses in the TITAN-II divertor coils (9.8 MW) are much smaller than those of the TITAN-I IBC divertor coils (120 MW). Also shown on the outboard view in Fig. 7 is the pumping aperture which leads to the vacuum tank surrounding the torus. This aperture is present for only the outboard 900 in poloidal angle; elsewhere shielding material protects the OH coils.

The results of the magnetics design of TITAN-II divertor (e.g., field-line connection length) were not sufficiently different from those of the TITAN-I to warrant a separate edge-plasma analysis. A summary of the results of the edge-plasma modeling for TITAN-I, which is also used for the TITAN-II design, is given in Table 5 and is described in detail in ref. [13]. The plasma power balance is controlled by the injection of a trace amount of a high atomic number impurity (xenon) into the plasma, causing strong radiation from the core plasma, the scrape-off layer (SOL) plasma, and the divertor plasma. About 95% of the steady-state heating power (alpha particle and ohmic heating by the current-drive system) is radiated to the first wall and divertor plate, with about 70% being radiated from the core plasma (i.e., inside the separatrix). This intense radiation reduces the power deposited on the divertor target by the plasma to an acceptably low level. Preliminary experimental results [14,15] suggest that beta-
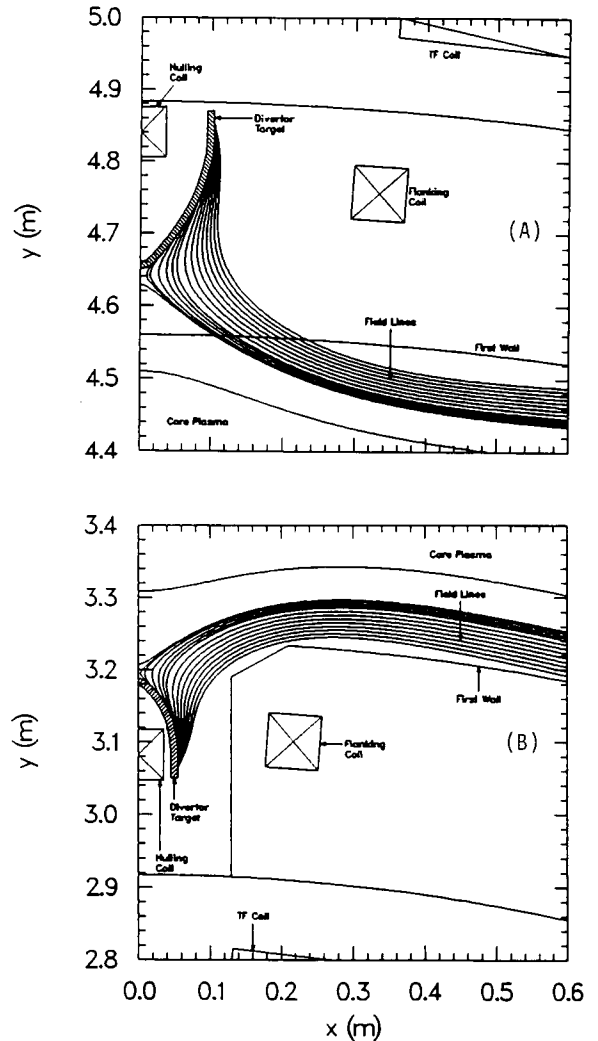

Fig. 7. Outboard (A) and inboard (B) equatorial-plane views of the divertor region for TITAN-II.

limited RFP plasmas can withstand a high fraction of power radiated without seriously affecting the operating point [13]. A further result of the radiative cooling is to reduce the electron temperature at the first wall and divertor target (also assisted by recycling) which reduces the sputtering-erosion problem.

To satisfy the requirement for a high-Z material for the plasma-facing surface of the divertor target, a tungsten-rhenium alloy (W–26Re) is used. The high rhenium content provides the high ductility and high strength necessary for the severe loading conditions. A single structural material is used for the divertor target to avoid the problem of bonding dissimilar materials

Table 5
Summary of TITAN-II edge-plasma conditions

Number of divertors	3
Scrape-off layer thickness	6 cm
Peak edge density	1.7×10^{20} m^{-3}
Peak edge ion temperature	380 eV
Peak edge electron temperature	220 eV
Plasma temperature at first wall	1.7 eV
Peak divertor density	6.0×10^{21} m^{-3}
Peak divertor plasma temperature	4.5 eV
Divertor recycling coefficient	0.995
Throughput of DT	6.7×10^{21} s^{-1}
Throughput of He	8.2×10^{20} s^{-1}
Vacuum tank pressure	20 mtorr

and of stress concentrations which occur at the interface of the two materials. The coolant tubes, therefore, are also made from W–26Re alloy.

The coolant for the divertor system is an aqueous LiNO$_3$ solution, as used in the TITAN-II blanket. Advantage is taken of the predicted differences in the physical properties of this solution compared with those of pure water to obtain the high critical heat fluxes (~ 16 MW/m^2) necessary to provide an adequate safety margin against burnout. The divertor-plate coolant flows in the toroidal/radial direction to equalize the power deposited on each tube, although this causes gaps between adjacent tubes (if they are of constant cross section) because of the double curvature of the divertor plate. Fabrication of the divertor target is based on brazing of the tungsten-alloy plate (which is produced by powder-metallurgy techniques) to a bank of constant cross-section coolant tubes, although alternative methods which allow tubes of variable cross section to be constructed, have also been considered.

Despite the intense radiation arising from the impurities injected into the plasma, careful shaping of the divertor target, as shown in Fig. 7, is also required to maintain the heat flux at acceptable levels at all points on the plate. Figure 8 shows the distribution of the various components of the surface heat flux along the divertor target for the inboard and outboard locations. The heat flux on the inboard and outboard targets are respectively, 7.5 and 5.8 MW/m^2 (compared with corresponding levels of 9.5 and 6.0 MW/m^2 for TITAN-I).

The temperature distribution of the divertor-plate coolant and structure is shown in Fig. 9. Given the heat loadings on the divertor-plate cooling tubes, the coolant conditions are determined by the requirements of obtaining an adequate safety factor on critical heat flux, and allowing the heat deposited into the divertor-target

cooling loop to be removed by a heat exchanger with the inlet coolant for the blanket. Additional constraints were that the coolant velocity should not exceed 20 m/s and that its composition should be the same as for the blanket (i.e., a lithium-atom percentage of 6.4%). These considerations led to the selection of the coolant-outlet conditions of 345°C and 14 MPa. At this pressure, the boiling point of a 6.4% LiNO$_3$ solution is 405°C, yielding a subcooling at the outlet conditions of
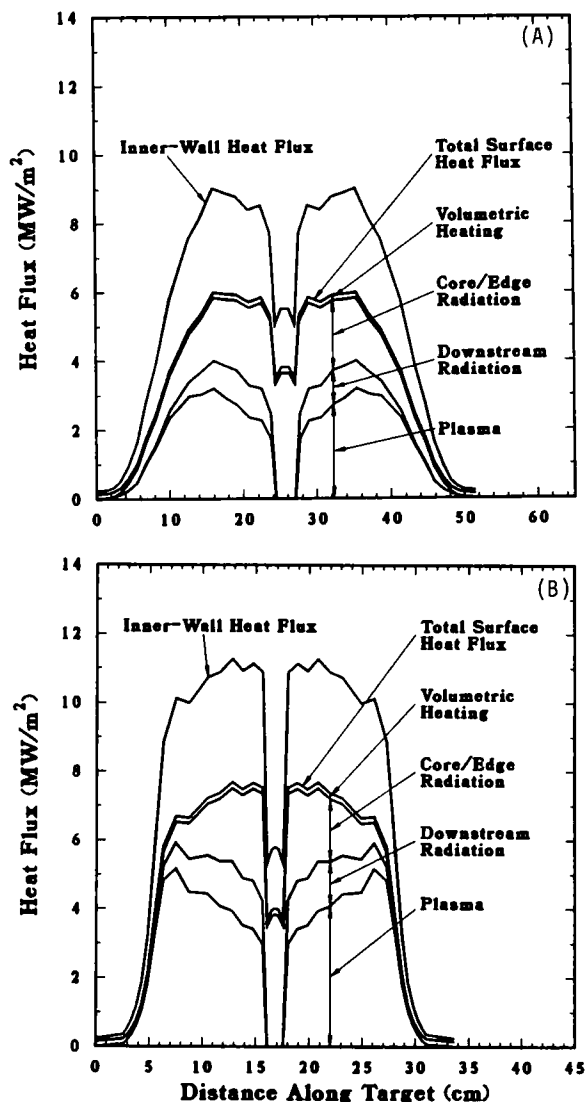

Fig. 8. Heat flux distribution on outboard (A) and inboard (B) sections of divertor target. The critical heat flux for TITAN-II divertor coolant is estimated at 16.2 MW/m^2. Distance along target is measured in the direction of coolant flow.
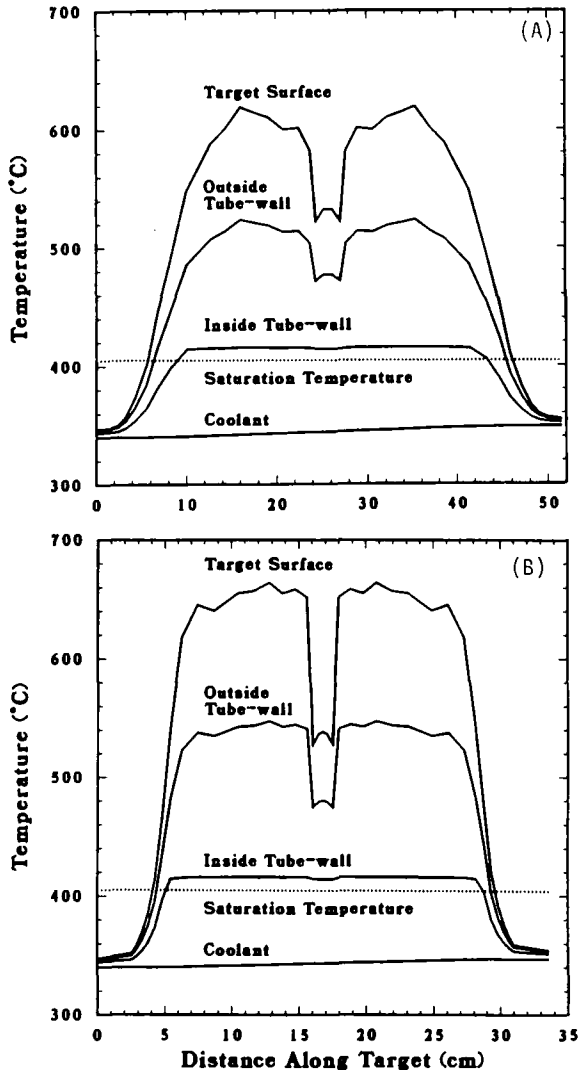
Fig. 9. Coolant and structure temperature distribution on outboard (A) and inboard (B) sections of the divertor target. Distance along target is measured in the direction of coolant flow.

60°C, and a critical heat flux of 16.2 MW/m² as predicted by the Jens and Lottes correlation [34]. A safety factor in excess of 1.4 with respect to critical heat flux is achieved at all points on the target; on the outboard target, where the heat fluxes are lower, the minimum safety factor is about 1.8.

The heat removed from the divertor plate is deposited into the blanket cooling circuit through a heat exchanger. In order to maintain a minimum temperature difference of 20°C in the heat exchanger between

the inlet divertor coolant and the inlet blanket coolant (298°C), the divertor-coolant inlet temperature must be not less than 318°C. For a divertor-coolant exit temperature of 345°C and temperature rise of about 7°C per pass, the TITAN-II divertor coolant passes four times across the target.

A 2-D finite-element analysis of the steady-state temperatures and stresses in the divertor was made using the finite-element code ANSYS [36]. This analysis indicated that the maximum equivalent thermal stress is about 500 MPa, within the allowable level of 600 MPa for tungsten. The thermal analysis showed that geometric effects concentrate the heat flux from its value on the plate surface to a higher value at the tube-coolant interface, and that the effects of the gaps between adjacent tubes in elevating structural temperatures are acceptable.

The vacuum system is based on the use of a large vacuum tank encompassing the entire torus, and connected to the divertor region by a duct located at each of the three divertor locations. Lubricant-free magnetic-suspension-bearing turbo-molecular pumps are proposed for the high-vacuum pumps to avoid the possibility of tritium contamination of oil lubricants. Pumps of the required size need to be developed.

9. Tritium systems

In TITAN-II design, the tritium is bred directly in the aqueous coolant of the primary heat-transport system. Tritium recovery and control of the tritium level in the primary coolant represent critical issues. In particular, tritium recovery from water is required on a scale larger than existing water-detritiation systems. However, considerable industrial experience with recovery of hydrogen and its isotopes from water is available, and some relevant process equipment is used on a larger scale in non-tritium applications.

The TITAN-II design has a higher tritium level (50 Ci/kg) in the primary-coolant water relative to previous design studies (e.g., 1 Ci/kg in BCSS [37]) in order to minimize the cost of water-processing equipment required for tritium recovery. This tritium level is possible for TITAN-II design because of: (1) a lower pressure in the primary system which is the result of the elevation of the fluid boiling point caused by the addition of the Li salt, (2) possible use of double-walled steam generators, (3) presence of the water pool which captures a large part of the tritiated-water leakage, (4) routine use of welded joints, and (5) removal of tritiated water to safe storage during major maintenance

Table 6
TITAN-II tritium inventories

System	T inventory (g)	Form
Primary-heat transport	1420 [a]	HTO
Beryllium	10	T in metal
Piping and structure	< 1	T in metal
Plasma chamber and vacuum	5	DT
Fuel processing	20	DT
Blanket tritium recovery	44	HTO
	550	HT
Shield	< 10	HTO
Tritium storage	1000	Metal tritide
Pool	940 [b]	HTO
TOTAL	4000	

[a] Based on 274 m^3 at 50 Ci/kg.
[b] Based on 22,640 m^3 at 0.4 Ci/kg.

operations. Component leakage rates and air-drier technology are based on CANDU systems performance [38]. The overall tritium-loss rate for the TITAN-II design is estimated at 50 Ci/d.

The tritium inventory in TITAN-II design is shown in Table 6. The total tritium inventory is four kilograms, roughly comparable to the inventory in some CANDU reactors at present. The largest inventory is in the primary circuit, which requires a larger blanket processing system.

The blanket tritium-recovery system reference design is summarized in Table 7. This system recovers 430 g/d of tritium, primarily through a five-stage vapor-phase catalytic-exchange (VPCE) system which transfers the tritium from the water to hydrogen gas, and then by cryogenic distillation for isotope separation. The TITAN-II FPC is submerged in the pool of water to achieve a high level of safety. The water pool

Table 7
TITAN-II blanket tritium-recovery system (based on extracting 465 g/d of T at 50 Ci/kg)

Maximum tritium concentration	50 Ci/kg in water
Tritium-extraction rate	465 g/d of T
Tritium inventory as water	44 g T
Tritium inventory as gas	550 g T
Blanket detritiation factor	93% per pass
Hydrogen-refrigeration power	5.7 MWe
Low-pressure steam to water distribution	5.7 MWth at 300 kPa
Low-pressure steam to VPCE	1.2 MWth at 600 kPa
High-pressure steam to VPCE	8.5 MWth at 2.5 MPa
Hydrogen-gas inventory	1500 kg
Building volume	36,000 m^3

contains tritium from primary-coolant system leakage, which is maintained at 0.37 Ci/kg by water distillation, with the enriched tritiated water from the distillation columns mixed with the primary-coolant water for final tritium recovery. The water-feed rate to the VPCE system is about 4000 kg/h at 50 Ci/kg. The estimated installed cost of the TITAN-II tritium recovery system is 130 M$ (1986), not including building, air cleanup, and indirect costs. Although the water-feed rate is about 10 times larger than the Darlington Tritium-Removal Facility, the cost is only 3 to 4 times larger because of the economy of scale, fewer VPCE stages, and the lower reflux ratio needed in the cryogenic columns by the light-water feed.

The other TITAN-II tritium-related systems and flow rates are also assessed. The fuel-processing systems are similar to those of TITAN-I, which are described in Reference [39]. Unique features include a redundant impurity-removal loop rather than relying on large tritium storage capacity, and a small feed to the isotope separation system because of the use of mixed DT fueling. Plasma-driven permeation is less important in TITAN-II than in TITAN-I because the first wall is at a lower temperature and is made of ferritic steel rather than vanadium. Back diffusion of protium is significant but acceptable. The air-detritiation system has a larger drier (but not recombiner) capacity to recover most of the tritiated water leaking from primary-system components.

The overall cost of the TITAN-II tritium system is 170 M$ (1986, installed). The cost is dominated by the blanket tritium-recovery system. Since tritium recovery in TITAN-II involves isotope separation of tritium from low concentrations in water, it is expected to be more expensive than for other fusion-blanket concepts. The present design approach is based on proven chemical exchange and distillation concepts. Costs for other tritium systems are similar to those for TITAN-I (except for a larger air-drier capacity). Some costs are estimated from ref. [40].

A major reduction in the costs and tritium levels requires a new water-detritiation approach. At present, laser separation is under investigation, but probably requires improvements in the lasers and optical materials to be attractive. Radiolysis might be helpful if a high yield of HT is obtained (not clear from present experiments), and if the associated O_2 production is acceptable.

Relative to the TITAN-I tritium system [39], the TITAN-II tritium system is more expensive, the total tritium inventory is larger, the overall tritium system is physically larger, and the chronic tritium releases are

larger. However, the TITAN-II tritium inventory is much less at risk for major release because of the lack of reactive chemicals, the low temperatures and pressures of most of the tritiated water, and the pool surrounding the FPC hot primary-coolant loop.

10. Safety design

Strong emphasis has been given to safety engineering in the TITAN study. Instead of an add-on safety design and analysis task, the safety activity was incorporated into the process of design selection and integration at the beginning of the study. The safety-design objectives of the TITAN-II design are: (1) to satisfy all safety-design criteria as specified by the U.S. Nuclear Regulatory Commission on accidental releases, occupational doses, and routine effluents; and (2) to aim for the best possible level of passive safety assurance.

The elevation view of TITAN-II reactor is shown in Fig. 1. The TITAN-II FPC is cooled by an aqueous lithium-salt solution and therefore the cooling circuit is a pressurized-water system. Furthermore, the primary coolant contains tritium at a high concentration of 50 Ci/kg. A passive safety system is thus required to handle different accident scenarios, to control the potential release of high-pressure primary coolant which contains tritium, and to prevent the release of induced radioactivities in the reactor structural materials even under the conditions of a loss-of-coolant-accident (LOCA).

The key safety feature of the TITAN-II design is the low-pressure, low-temperature water pool that surrounds the fusion power core and the entire primary-coolant system (Fig. 1). In the case of a major coolant-pipe break, the pressurized coolant in the hot loop will mix with the pool of water since the complete primary loop is in the pool. With this mixing, the temperature of the pool would only rise moderately because of the much larger volume of the water pool. In fact, even if the heat transfer from the pool to the surrounding earth is ignored, it would take more than seven weeks for the temperature of the water pool to reach 100°C. Therefore, the cold pool of water acts as a heat sink to dilute the reactor thermal and decay afterheat energy and also eliminates the possibility of releasing tritiated water vapor or other radioactive material to the environment.

Based on the "loop-in-pool" concept of the TITAN-II design, different scenarios for handling normal and off-normal situations were evaluated. The size and operating conditions of the TITAN-II water pool are determined by these analyses. In the TITAN-II design, the primary-cooling circuit is not completely insulated from the pool, so the pool can absorb the decay afterheat power in case of a loss-of-flow accident (LOFA) in either the primary circuit or the steam generators. This power is then removed by separate heat exchangers in the pool. The pool temperature should be kept as low as possible to maintain an adequate heat-sink capability in the pool in case of an accident. On the other hand, the pool temperature should be reasonably high so that the size of the afterheat-removal heat exchangers in the pool, which are capable of removing the steady power of 34 MW, can be minimized. The exact pool temperature should be determined by detailed design. For the TITAN-II reactor, a pool temperature range of 60 to 70°C is found to be reasonable based on detailed evaluation of the accident scenarios.

A potential accident for pressurized-water systems is a double-ended rupture of a main coolant line. The escaping jet of the primary coolant (as steam), which may contain radioactive material, will raise the pressure inside the primary containment building and may result in the release of radioactivity to the environment. Another advantage of the TITAN-II water pool surrounding the FPC is the potential to suppress the consequences of a double-ended rupture of the primary-coolant circuit by containing the escaping jet of the primary coolant inside the water pool. The analysis shows that for a double-ended rupture of a 0.5-m-diameter hot leg, at least 6 to 7 m of cold (60°C), fully degassed water is needed above the break to prevent a direct discharge of steam into the containment building. This figure has been used to determine the minimum height of TITAN-II pool.

Two of the major accidents postulated for the FPC are the LOFA and LOCA. Thermal responses of the TITAN-II FPC to these accidents are modeled using a finite-element heat-conduction code, TACO2D [41]. Analysis of a LOCA without the pool showed that the peak temperature of the ferritic steel and beryllium would exceed the melting point of these materials. The necessity of the low-pressure pool is evident from these results.

Figure 10 shows the temperature of the TITAN-II FPC as a function of time after the initiation of a LOFA (with the pool). For this accident scenario, very little temperature excursion is observed, primarily because of the presence of natural convection within the pool and the primary loop. The first-wall peak temperature of 348°C is reached after 355 seconds. The TITAN-II reactor appears to be capable of withstanding the loading conditions of this accident scenario.

The thermal response of the TITAN-II FPC to a LOCA with the low-pressure pool is also studied. The accident is assumed to be initiated with a guillotine break in the primary cold leg, below the level of the torus. At the onset of the accident, a very rapid (~ 1 s) de-pressurization of the primary loop occurs until the primary-loop pressure reaches the saturation pressure of the primary coolant. Following the initial de-pressurization to saturation conditions, a slower de-pressurization takes place until the primary loop and the pool are at equal pressure. Choked flow at the pipe break determines the rate of de-pressurization. As the pressure in the primary loop drops below the saturation pressure of the primary coolant, flashing of the primary coolant occurs, and the sudden volume change forces the coolant out of the pipe break (blow-down phase). The blow-down phase in typical design-basis accidents for PWRs lasts 10 to 20 seconds, provided that no emergency core-cooling system is engaged. If the pipe break occurs at the lowest point of the primary loop (i.e., the worst case accident) any steam that forms inside the primary piping is trapped because of the buoyancy force. For accident analysis of the TITAN-II FPC, it is conservatively assumed that at the end of blow-down phase, the entire primary loop will be filled with 330°C steam (operating conditions).

During the re-flood phase, heat is lost from the primary loop (steam) to the surrounding pool and the steam trapped in the primary loop begins to condense. The condensation rate depends on many variables; for this analysis, it is assumed that this phase would last 5 minutes. Virtually any condensation rate can be designed into the system simply by adding insulation to the piping (decreasing the rate of condensation), or by
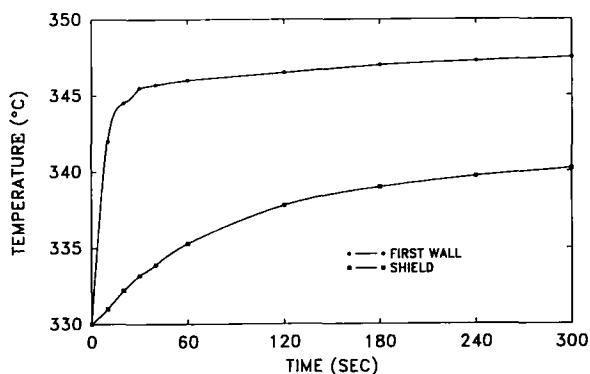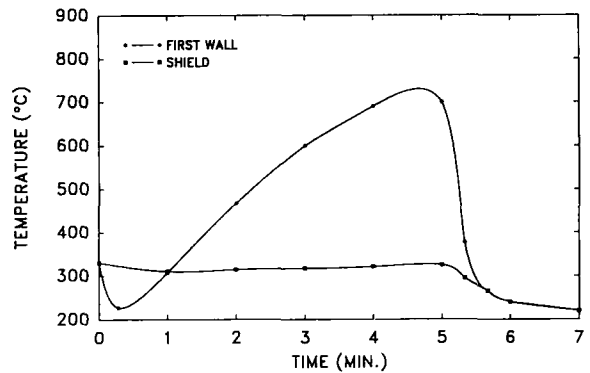

Fig. 11. The thermal response of the TITAN-II FPC to a LOCA with the low-pressure pool as a function of time after the initiation of the accident (with a re-flood time of 300 s).

exposing more primary piping to the pool water (increasing the rate of condensation). The final phase of the accident is the onset of natural circulation.

Thermal response of the TITAN-II fusion power core to this accident scenario is shown in Fig. 11. The peak temperature of the FPC is 732°C which is 688°C below the melting point of the ferritic steels. The peak beryllium temperature is 481°C, which is 802°C below its melting point.

The key safety feature of the TITAN-II design is the low-pressure, low-temperature water pool that surrounds the FPC. Detailed safety analyses have been performed which show that the TITAN-II pool can contain the thermal and afterheat energy of the FPC and will remain at a low enough temperature so that tritium or other radioactive material in the primary-coolant system will not be released. Therefore, the public safety is assured by maintaining the integrity of the water pool. Since the water-pool structure can be considered a large-scale geometry, the TITAN-II design can be rated as a level-2 of safety assurance design [42,43]. The potential safety concerns are the control of routine tritium releases and the handling of ^{14}C waste, which is generated from the nitrogen in the $LiNO_3$ salt.

Plasma-accident scenarios need to be further evaluated as the physics behavior of RFPs becomes better understood. Preliminary results indicate that passive safety features can be incorporated into the design so that the accidental release of plasma and magnetic energies can be distributed without leading to major releases of radioactivity. Activities in this area need to be continued, especially for high-power-density devices. It should be pointed out that for the TITAN-II

Fig. 10. The thermal response of the TITAN-II FPC to a LOFA with the low-pressure pool as a function of time after the initiation of the accident.

design, plasma-related accidents are of concern from the consideration of investment protection and would have minimum impact on public safety. This characteristic is again a result of the presence of the large pool of water that allows the passive protection of the public.

11. Waste disposal

The neutron fluxes calculated for the reference TITAN-II reactor were used as the input to the activation calculation code, REAC [44]. These results were analyzed to obtain the allowable concentrations of alloying and impurity elements in the TITAN-II FPC components. Waste-disposal analysis has shown that the compact, high-power-density TITAN-II reactor can be designed to meet the criteria for Class-C waste disposal [45]. The key features for achieving Class-C waste in the TITAN-II reactor are attributed to: (1) materials selection and (2) control of impurity elements.

The first-wall, blanket, and shield components of the TITAN-II reactor are all integrated in a one-piece lobe design and are all replaced every year. Therefore, one may estimate the allowable concentration levels of the impurity elements by averaging over all components in the lobe. The maximum allowable impurity concentration in the "averaged" TITAN-II FPC are

Table 8
Waste-disposal-ratings for the "averaged" TITAN-II blanket [a]

Element	Present case		Controlled case	
	Nominal level [b] (appm)	Class-C Rating	Controlled level (appm)	Class-C Rating
Nb	0.1% [c]	8.33	1.0 [d]	0.42
Mo	1.0% [c]	0.27	6.0 [d]	0.30
Ag	1.0	0.054	0.07	0.054
Tb	5.0	1.06	0.1 [d]	0.10
Ir	5.0	0.0077	0.001	0.0077
W	0.9% [c,e]	0.081	0.9% [e]	0.081
TOTAL		9.78		0.96

[a] Based on operation at 18 MW/m² of neutron wall loading for 1 FPY. Note that a conservative lifetime fluence value of 15 MWy/m² is used for the TITAN-II reference design (0.8 FPY at 18 MW/m²).

[b] From ref. [37].

[c] Concentrations in atomic percentage.

[d] Controlled levels lower than impurity levels in ferritic steel.

[e] Present tungsten content in the reduced-activation ferritic steel.

shown in Table 8. It appears that the concentration limits for all these impurity elements, except niobium and terbium, are readily achievable for the averaged

Table 9
Summary of TITAN-II reactor materials and related waste quantities for Class-C waste disposal [a]

Component	Material	Lifetime (FPY) [a]	Volume (m³)	Weight (tonne)	Annual replacement mass (tonne/FPY)
First wall	Ferritic steel (9-C)	1	0.26	2.0	2.0
Be zone	Ferritic steel (9-C)	1	2.5	19.7	19.7
Breeder zone	Ferritic steel (9-C)	1	2.0	15.3	15.3
Shield	Ferritic steel (9-C)	1	3.9	30.5	30.5
TF coils	Modified steel		0.54	4.8	0.08
	Copper		3.8	34.0	1.13
	Spinel		0.54	2.2	0.08
	TOTAL	30	4.9	41.0	1.39
OH coils	Modified steel		5.4	49.0	1.63
	Copper		38.2	342.0	11.4
	Spinel		5.4	23.0	0.77
	TOTAL	30	49.0	414.0	13.8
EF coils shield	Modified steel	30	5.6	50.0	1.7
Divertor shield	Ferritic steel	1	0.48	3.78	3.78
TOTAL CLASS-C WASTE (lifetime)			334.0	2643.0	88.1

[a] Based on operation at 18 MW/m² of neutron wall loading for 1 FPY. Note that a conservative lifetime fluence value of 15 MWy/m² is used for the TITAN-II reference design (0.8 FPY at 18 MW/m²).

TITAN-II FPC. Careful impurity control processes are necessary for Nb and Tb when the structural alloy is fabricated.

The reduced-activation ferritic steel (9-C) used as structural material for the TITAN-II reactor contains tungsten as one of the important alloying elements replacing molybdenum which is an undesirable element for Class-C waste disposal. However, the tungsten content should also be controlled because of the production of a second-step reaction daughter radionuclide, ^{186m}Re (with a half-life of 200,000 years). The "averaged" allowable concentration level of tungsten is 11.0%, more than two orders of magnitude larger than the present tungsten level in the reduced-activation ferritic steels (0.89%).

Assuming that the structural alloy meets all required levels of impurity and alloying elements as shown in the controlled case in Table 8, estimates are made for the TITAN-II reactor materials and related waste quantities for Class-C disposal. The divertor-shield coverage is taken as 13% in the TITAN-II design, identical to the TITAN-I design. The results are presented in Table 9. The annual replacement mass of TITAN-II FPC is estimated at about 71 tonne/FPY (9.1 m^3), assuming that the entire blanket lobe and the divertor shield are replaced every FPY. The data in Table 9 is for a modified TITAN-II design with a 0.03-m shield and a 0.17-m blanket breeder zone, rather than the 0.1-m shield and 0.1-m blanket breeder zone of the reference design. The reduced shield thickness in this design will decrease the annual replacement mass by about 50 tonne/FPY and also satisfies the structural-design aspects of the blanket lobe. The penalty for this modified design is a 1.5% reduction in the blanket energy multiplication.

The TITAN-II divertor plates are fabricated with a tungsten armor because of its low sputtering properties. The waste-disposal rating of the divertor plates is estimated to be a factor of 10 higher than for Class-C disposal after one year of operation. The annual replacement mass of this non-Class-C waste is about 0.35 tonne/FPY, about 0.4% of the annual replacement mass.

Because of the nitrate salt dissolved in the aqueous-solution coolant, the TITAN-II reactor is also producing ^{14}C from ^{14}N (n, p) reactions. The annual production rate of ^{14}C is about 5.2×10^4 Ci. Using the present 10CFR61 regulations, where the allowable concentration of ^{14}C for Class-C disposal is 8 Ci/m^3 and if ^{14}C remains in the aqueous-solution coolant, the coolant should be replaced at a rate of 7×10^3 tonne/FPY (6.5×10^3 m^3). The replacement mass of

the coolant can be reduced to about 80 tonne/FPY, if Fetter's evaluation [46] is used as the limiting value (700 Ci/m^3). Because of the large quantities of aqueous solution to be disposed of annually and uncertainties in the transport of the ^{14}C isotope in the primary loop, extraction of the ^{14}C activity from the coolant and disposal of the concentrated quantity as non-Class-C waste should be considered.

The safety and environmental conclusions derived from the TITAN reactor study are general, and provide strong indications that Class-C waste disposal can be achieved for other high-power-density approaches to fusion. These conclusions also depend on the acceptance of recent evaluations of limiting-specific activities carried out under 10CFR61 methodologies [46].

12. Maintenance

The TITAN reactors are compact, high-power-density designs. The small physical size of these reactors permits each design to be made of only a few pieces, allowing a single-piece maintenance approach [7,8]. Single-piece maintenance refers to a procedure in which all of components that must be changed during the scheduled maintenance are replaced as a single unit, although the actual maintenance procedure may involve the movement, storage, and reinstallation of some other reactor components. The entire reactor torus in both TITAN designs is replaced as a single unit during scheduled maintenance. Also, because of the small physical size and mass of the TITAN-II FPC, the maintenance procedures can be carried out by vertical lifts, allowing a much smaller reactor vault.

Potential advantages of single-piece maintenance procedures are identified:

(1) Shortest period of downtime resulting from scheduled and unscheduled FPC repairs;
(2) Improved reliability resulting from integrated FPC pretesting in an on-site, non-nuclear test facility where coolant leaks, coil alignment, thermal-expansion effects, etc., would be corrected by using rapid and inexpensive hands-on repair procedures prior to committing the FPC to nuclear service;
(3) No adverse effects resulting from the interaction of new materials operating in parallel with radiation-exposed materials;
(4) Ability to modify continually the FPC as may be indicated or desired by reactor performance and technological developments; and
(5) Recovery from unscheduled events would be more standard and rapid. The entire reactor torus is

replaced and the reactor is brought back on line with the repair work being performed, afterwards, outside the reactor vault.

The lifetime of the TITAN-II reactor torus (including the first wall, blanket, and divertor modules) is estimated to be in the range of 15 to 18 MWy/m^2, and the more conservative value of 15 MWy/m^2 will require the change-out of the reactor torus on a yearly basis for operation at 18 MW/m^2 of neutron wall loading at 76% availability. The TF coils can last for the entire plant life. However, during the maintenance procedure, the TF coils are not separated from the reactor torus and are replaced each year. After the completion of the maintenance procedure, the TF coils can be separated from the reactor torus and reused at a later time. The impact of discarding (not reusing) the TF coils annually is negligible on the COE. The choice between reusing or discarding the TF coils requires a detailed consideration of: (1) activation intensity of the reused TF coils, (2) remote assembly of activated TF coils to a "clean" FPC, and (3) additional waste generated if TF coils are discarded annually.

Fourteen principal tasks must be accomplished for the annual, scheduled maintenance of the TITAN-II fusion power core. These steps are listed in Table 10. Tasks that will require a longer time to complete in a modular design are also identified in Table 10 (assuming the same configuration for the modular design as that of TITAN-II). Vertical lifts have been chosen for the component movements during maintenance. Lift limits for conventional bridge cranes is around 500 tonnes, with special-order crane capacities in excess of 1000 tonnes. The most massive components lifted during TITAN-II maintenance are the reactor torus (180 tonnes) and the upper OH-coil set (OH coils 2 through 4) and its support structure (120 tonnes), which are easily manageable by the conventional cranes.

An important feature of the TITAN design is the pretest facility. This facility allows the new torus assemblies to be tested fully in a non-nuclear environment prior to committing it to full-power operation in the reactor vault. Any faults discovered during pretesting can be quickly repaired using inexpensive hands-on maintenance. Furthermore, additional testing can be used as a shakedown period to reduce the infant mortality rate of the new assemblies. A comprehensive pretest program could greatly increase the reliability of the FPC, hence increasing the overall plant availability. These benefits of pretesting (higher reliability, higher availability) must be balanced with the additional cost associated with the pretest facility. The more representative the pretests are of the actual operation, the

Table 10
Principal tasks during the TITAN-II maintenance procedure

1. Orderly shutdown of the plasma and discharge of the magnets
2. Continue cooling the FPC at a reduced level until the decay heat is sufficiently low to allow natural convection cooling in the atmosphere
3. During the cool-down period
   a. Continue vacuum pumping until sufficient tritium is removed from the FPC,
   b. Valve-off all systems which will be disconnected during maintenance (i.e., vacuum and electrical systems) and, depending on the maintenance method, drain the water pool above the FPC,
   c. Disconnect electrical and coolant supplies from the upper OH-coil set,
   d. Break vacuum
4. Drain primary coolant from FPC
5. Lift OH-coil set and store in the lay-down area
6. Disconnect primary-coolant supplies at ring headers [a]
7. Lift the reactor torus and move to the hot cell [a]
8. Inspect FPC area ·
9. Install the new, pretested torus assembly [a]
10. Connect primary-coolant supplies, TF-coil electrical supplies, and re-weld all vacuum ducts [a]
11. Replace the upper OH-coil set and connect electrical and coolant supplies
12. Hot test the FPC [b]
13. Pump-down the system
14. Initiate plasma operations

[a] The time required to complete these tasks is likely to be longer for a modular system than for a single-piece system, assuming similar configuration.

[b] The new torus assembly is pretested and aligned before committment to service. Only minimum hot testing would be required.

more duplication of the primary-loop components is required.

13. Summary and key technical issues

The TITAN reversed-field-pinch (RFP) fusion reactor study [1] is a multi-institutional research effort to determine the technical feasibility and key developmental issues for an RFP fusion reactor operating at high power density and to determine the potential economic (cost of electricity, COE), operational (maintenance and availability), safety, and environmental features of high mass-power-density (MPD) fusion systems.

Two different detailed designs, TITAN-I and TITAN-II, have been produced to demonstrate the possibility of multiple engineering design approaches to high-MPD reactors. Both designs would use RFP plasmas operating with essentially the same parameters. The major features of the designs are listed in Table 1. Both conceptual reactors are based on the DT fuel cycle, have a net electric output of about 1000 MWe, are compact and have a high mass power density of about 800 kWe/tonne of fusion power core (FPC). The mass power density and the FPC power density of several fusion reactor designs and a fission pressurized-water reactor (PWR) are shown in Fig. 7 on p. 77 of the Introduction by F. Najmabadi and compared with those of the TITAN reactors. The TITAN study further shows that with proper choice of materials and FPC configuration, compact reactors can be made passively safe and that the potential attractive safety and environmental features of fusion need not be sacrificed in compact reactors. The TITAN designs would meet the U.S. criteria for the near-surface disposal of radioactive waste (Class-C, 10CFR61) [45] and achieve a high level of safety assurance [42,43] with respect to FPC damage by decay afterheat and radioactivity release caused by accidents. Very importantly, a "single-piece" FPC maintenance procedure, unique to high-MPD reactors, has been worked out and appears feasible for both designs.

Parametric system studies have been used to find cost-optimized designs, to determine the parametric design window associated with each approach, and to assess the sensitivity of the designs to a wide range of physics and engineering requirements and assumptions. The design window for such compact RFP reactors would include machines with neutron wall loadings in the range of 10 to 20 MW/m^2 with a shallow minimum for COE at about 19 MW/m^2. The high MPD values possible for the RFP appear to be a unique attribute of this confinement concept [6]. Reactors in this "design window" are physically small and a potential benefit of this "compactness" is improved economics. Also, the cost of the FPC for TITAN reactors is a small fraction of the overall estimated plant cost (< 10%, similar to a PWR), making the economics of the reactor less sensitive to changes in the plasma performance or unit costs for FPC components. Moreover, since the FPC is smaller and cheaper, a development program should cost less. Even though operation at the lower end of the this range of wall loading (10 to 12 MW/m^2) is possible, and may be preferable, the TITAN study adopted the design point at the upper end (18 MW/m^2) in order to quantify and assess the technical feasibility and physics limits for such high-MPD reactors.

The TITAN-II FPC is a self-cooled aqueous "loop-in-pool" design with a dissolved Li salt (LiNO$_3$ with 6.4 at% lithium) as the breeder. The structural material is ferritic-steel alloy, 9-C [19] (a reduced-activation high-strength alloy, 12Cr-0.3V-1W-6.5Mn-0.08C). The first-wall and blanket lobes are integrated and contain the pressurized coolant at 7 MPa. The structural load from the pressurized lobes is supported by a welded two-piece shield which forms a blanket container packing several lobes into a blanket sector. Three toroidal divertor chambers divide the reactor torus into three sectors. The coolant enters the lobes from the bottom, flows around the torus poloidally, and exits through the top plena. Subcooled-flow-boiling heat transfer is needed to cool the first wall. The blanket contains beryllium rods with ferritic-steel alloy 9-C cladding as the neutron multiplier.

Both lithium-hydroxide (LiOH) and lithium nitrate (LiNO$_3$) salts were considered because they are highly soluable in water. The LiNO$_3$ solution is selected as the reference breeding material because: (1) LiOH is more corrosive and (2) radiolytic decomposition of water which results in the formation of highly corrosive substances is minimized when nitrate salts are added to water. Account is taken of the thermophysical properties of the salt solution, which are significantly different from those of the pure water. The TITAN-II tritium-control and extraction system would be, in principle, an extension of the technology developed by the Canadian CANDU fission reactor program [38].

A key feature of TITAN-II is that the FPC and the entire primary loop are submerged in a pool of low-temperature, low-pressure water. The basic sources of thermal energy after reactor shutdown are from the hot loop and the induced afterheat from the torus first wall and blanket structures. The first-wall and blanket coolant-channel configurations are designed to allow natural circulation to develop in the case of a loss-of-flow accident. In the case of a major break in the primary coolant pipes, the cold pool would absorb the thermal and afterheat energy from the hot loop. Calculations show that the pool remains at a sufficiently low temperature to prevent the release of tritium or other radioactivity in the blanket coolant system. As such, the TITAN-II design appears to achieve complete passive safety (level 2 of safety assurance [42,43]).

The general arrangement of the TITAN-II reactor is illustrated in Figs. 1–3 of this paper and Figs. 4 and 5 of the Introduction by F. Najmabadi on p. 74. The operational (maintenance and availability), safety, and

environmental issues have been taken into account throughout the design. For example, the size of the expensive containment building is reduced because all maintenance procedures would be performed by vertical lift of the components (heaviest component weighs about 180 tonnes). The compactness of the TITAN designs would reduce the FPC to a few small and relatively low-mass components, making toroidal segmentation unnecessary. A "single-piece" FPC maintenance procedure, in which the first wall and blanket are removed and replaced as a single unit is, therefore, possible. This unique approach permits the complete FPC to be made of a few factory-fabricated pieces, assembled on site into a single torus, and tested to full operational conditions before installation in the reactor vault. The low cost of the FPC means a complete, "ready-for-operation" unit be can be kept on site for replacement in case of unscheduled events. All of these features are expected to improve the plant availability.

The results from the TITAN study support the technical feasibility, economic incentive, and operational attractiveness of compact, high mass-power-density RFP reactors. The road towards compact RFP reactors, however, contains major challenges and uncertainties, and many critical issues remain to be resolved. The TITAN study has identified the key physics and engineering issues which are central to achieving reactors with the features of TITAN-I and TITAN-II.

The experimental and theoretical bases for RFPs have grown rapidly during the last few years [6], but a large degree of extrapolation to TITAN-class reactors is still required. The degree of extrapolation is one to two orders of magnitude in plasma current and temperature and two to three orders of magnitude in energy confinement time. However, the TITAN plasma density, poloidal beta, and plasma current density all are close to present-day experimental achievements. The next generation of RFP experiments [15,47] with hotter plasmas will extend the data base toward reactor-relevant regimes of operation. The TITAN study has brought out and illuminated a number of key physics issues, some of which require greater attention from the RFP physics community. These issues are discussed in ref. [2].

The physics of confinement scaling, plasma transport, and the role of the conducting shell are already major efforts in RFP research. However, the TITAN study points to three other major issues. First, operating high-power-density fusion reactors with intensely radiating plasmas is crucial. Confirming that the global energy confinement time remains relatively unaffected while core-plasma radiation increases (a possible

unique feature of RFP) is extremely important. Second, the TITAN study has adopted the use of three "open-geometry" toroidal divertors as the impurity control and particle exhaust system. Even with an intensely radiative plasma, using an array of poloidal pump-limiters as the impurity-control system would suffer from the serious erosion of the limiter blades (and possibly the first wall). The physics of toroidal-field divertors in RFPs must be examined, and the impact of the magnetic separatrix on RFP confinement must be studied. If toroidal divertors are consistent with confinement and stability in RFPs, then high-recycling divertors and the predicted high-density, low-temperature scrape-off layer must be also confirmed. Third, early work in the TITAN study convinced the team that high mass-power-density, compact RFP reactors must operate at steady state. Current drive by magnetic-helicity injection utilizing the natural relaxation process in RFP plasma is predicted to be efficient [10,11] but experiments on oscillating-field current drive (OFCD) are inconclusive. Testing OFCD in higher temperature plasmas must await the next generation of RFP experiments, namely ZTH [15] and RFX [47].

The key engineering issues for TITAN-II FPC have been discussed. In the area of materials, more data on irradiation behavior (especially hydrogen embrittlement) of the ferritic-steel alloy, 9-C, are needed to confirm the materials prediction and accurately estimate the lifetime of TITAN-II first wall. The compatibility of ferritic steels with concentrated $LiNO_3$ solution is an important issue. Even though some experimental data do not show high corrosion rates or high susceptibility of stress-corrosion cracking, a research effort is needed to confirm these results in a fusion environment. The effects of radiolytic decomposition products and high-energy neutron irradiation on corrosion mechanisms and rates should be determined. Ceramic insulators offer the potential of minimum irradiation-induced conductivity, high melting and decomposition temperatures, retention of strength, and minimum irradiation-induced swelling. Further experimental data on irradiation behavior of these insulators are needed.

The physical properties of the concentrated $LiNO_3$ salt solution are very different from those of pure water. The exact coolant conditions should be considered in designing the blanket. The thermal-hydraulic design of the FPC can take advantage of the differences in the properties of the concentrated solution, for example, by reducing the coolant pressure or increasing the temperature without incurring an increased risk of burnout. A much expanded experimental data base is required for the salts and conditions

proposed before the thermal performance of an aqueous-salt blanket at high temperatures and heat fluxes can be confidently predicted.

The design of the impurity-control system poses some of the most severe problems of any component of a DT fusion reactor; for a compact or high-power-density design, these problems can be particularly challenging. Physics operation of high-recycling toroidal-field divertors in RFPs should be experimentally demonstrated and the impact of OFCD on the divertor performance studied. Cooling of the TITAN-II divertor plate requires experimental data on heat-transfer capabilities of concentrated-salt solutions, as outlined above. Fabrication of the tungsten divertor plate remains to be demonstrated and the degree of precision needed for target shaping and control of the position of the plasma separatrix are particularly difficult tasks.

A key concern for the aqueous blanket design is the area of tritium extraction and control. The overall cost of the TITAN-II tritium-recovery system is 170 M$. A major reduction in the costs and tritium levels requires a new water-detritiation approach. At present, laser isotope separation is under investigation but probably requires improvements in the laser and optical material to be attractive. Radiolysis might be helpful if a high yield of HT is obtained which is not clear from present experiments, and if the associated production of oxygen is acceptable.

In summary, the results from the TITAN study support the technical feasibility, eoonomic incentive, and operational attractiveness of compact, high-mass-power-density RFP reactors. It must be emphasized, nevertheless, that in high-power-density designs such as TITAN, the in-vessel components (e.g., first wall and divertor plates) are subject to high surface heat fluxes and that their design remains the most difficult engineering challenge. Also, the RFP plasma itself must operate in the manner outlined: with toroidal-field divertors, with a highly radiative core plasma, and at steady state. Future research will determine if, in fact, the physics and technology requirements of TITAN-like RFP reactors are achievable.

Acknowledgements

References

[1] F. Najmabadi, N.M. Ghoniem, R.W. Conn, et al., The TITAN Reversed-Field Pinch Reactor Study, Scoping Phase Report, joint report of University of California Los Angeles, General Atomics, Los Alamos National Laboratory, and Rensselaer Polytechnic Institute, UCLA-PPG-1100 (1987).

[2] R.W. Conn (chairman and editor), Magnetic Fusion Advisory Committee Panel X Report on High Power Density Fusion Systems (May 8, 1985).

[3] J. Sheffield, R.A. Dory, S.M. Cohn, J.G. Delene, L.F. Parsley, et al., Cost assessment of a generic magnetic fusion reactor, Oak Ridge National Laboratory report ORNL/TM-9311 (1986) 103.

[4] R.A. Krakowski, R.L. Miller, and R.L. Hagenson, The need and prospect for improved fusion reactors, J. Fusion Energy 5 (1986) 213.

[5] R.A. Krakowski, R.L. Hagenson, N.M. Schnurr, C. Copenhaver, C.G. Bathke, R.L. Miller, and M.J. Embrechts, Compact Reversed-Field Pinch Reactors (CRFPR), Nucl. Eng. Design/Fusion 4 (1986) 75.

[6] H.A. Bodin, R.A. Krakowski, and O. Ortolani, The Reversed-Field Pinch: from experiment to reactor, Fusion Technol. 10 (1986) 307.

[7] R.L. Hagenson, R.A. Krakowski, C.G. Bathke, R.L. Miller, M.J. Embrechts, et al., Compact Reversed-Field Pinch Reactors (CRFPR): Preliminary engineering considerations, Los Alamos National Laboratory report LA-10200-MS (1984).

[8] C. Copenhaver, R.A. Krakowski, N.M. Schnurr, R.L. Miller, C.G. Bathke, et al., Compact Reversed-Field Pinch Reactors (CRFPR), Los Alamos National Laboratory report LA-10500-MS (1985).

[9] R.L. Miller, Systems studies paper, Fusion Engrg. Des. (to be published).

[10] M.K. Bevir and J.W. Gray, Relaxation, flux consumption and quasi steady state pinches, Proc. of RFP Theory Workshop, Los Alamos, NM, USA (1980), Los Alamos National Laboratory report LA-8944-C (1982) 176.

[11] K.F. Schoenberg, J.C. Ingraham, C.P. Munson, et al., Oscillating-field current-drive experiments in a reversed-field pinch, Phys. Fluids 8 (1989) 2285; also R.A. Scardovelli, R.A. Nebel, and K.A. Werley, Transport simulation of the oscillating field current drive experiment in the Z-40M, Los Alamos National Laboratory report LA-UR-2802 (1988).

[12] J.B. Taylor, Relaxation and magnetic reconnection in plasma, Rev. Mod. Phys. 58 (1986) 741; also: Relaxation of toroidal plasma and generation of reversed magnetic fields, Phys. Rev. Lett. 33 (1974) 1139; and: Relaxation of toroidal discharges, Proc. 3rd Topical Conf on Pulsed

High-Beta Plasmas, Abingdon, September 1975 (Pergamon Press, London, 1976) 59.

[13] F. Najmabadi, Divertors ..., Fusion Engrg. Des. 23 (1993), in this issue.

[14] M.M. Pickrell, J.A. Phillips, C.J. Buchenauer, T. Cayton, J.N. Downing, A. Haberstich, et al., Evidence for a poloidal beta limit on ZT-40M, Bull. Am. Phys. Soc. 29 (1984) 1403.

[15] P. Thullen and K. Schoenberg (Eds.), ZT-H reversed-field pinch experiment technical proposal, Los Alamos National Laboratory report LA-UR-84-2602 (1984) 26.

[16] F. Najmabadi, Physics of TITAN ..., Fusion Engrg. Des. 23 (1993), in this issue.

[17] C. Bathke, TITAN Magnetics and OFCD, Fusion Engrg. Des. 23 (1993), in this issue.

[18] C.P.C. Wong, TITAN-II Safety, Fusion Engrg. Des. 23 (1993), in this issue.

[19] D.S. Gelles, N.M. Ghoniem, and R.W. Powell, Low activation ferritic alloys patent description, University of California Los Angeles report UCLA/ENG-87-9 PPG-1049 (1987).

[20] D. Steiner et al., A heavy water breeding blanket, Proc. 11th Symp. on Fusion Engineering, Austin, TX (1985).

[21] S. Sharafat, TITAN Materials ..., Fusion Engrg. Des. 23 (1993), in this issue.

[22] W.F. Bogaerts, M.J. Embrechts, and R. Waeben, Application of the aqueous self-cooled blanket concept to a tritium producing shielding blanket for NET, University of Leuven (Belgium) report EUR-FU/XII-80/87/75 (1987).

[23] D.N. Braski, The effect of neutron irradiation on the tensile properties and microstructure of several vanadium alloys, Proc. ASTM Conf. on Fusion Reactor Materials, Seattle, WA (1986).

[24] E.T. Cheng and R.W. Conn, Waste disposal ratings in the TITAN RFP reactor, Proc. IEEE 12th Symp. on Fusion Engineering, Monterey, CA (October 1987) 913.

[25] R. Waeben, W. Bogaert, and M. Embrecht, Initial corrosion evaluation of candidate materials for an ASCB driver blanket for NET, Proc. IEEE 12th Symp. Fusion Engineering, Monterey, CA (October 1987) 1332.

[26] R.S. Treseder, Guarding against hydrogen embrittlement, Chem. Engrg. 29 (1981) 105.

[27] M.G. Fontana and N.D. Greene, Corrosion Engineering (McGraw-Hill International Book Company, Singapore, 1978).

[28] Steels for hydrogen service at elevated temperatures and pressures in petroleum refineries and petrochemical plants, API Publication 941, 2nd edition (1971).

[29] R.H. Wood, University of Delaware, Newark, personal communication (August 1987).

[30] T.J. McCarville, D.H. Berwald, W. Wolfer, F.J. Fulton, J.D. Lee, et al., Technical issues for beryllium use in fusion blanket applications, Lawrence Livermore National Laboratory report UCID-20319 (1985).

[31] W.W. Engle, Jr., A User's Manual for ANISN, a one-dimensional discrete ordinates transport code with

[32] anisotropic scattering, Oak Ridge Gaseous Diffusion Plant report K-1693 (1967).

[32] R. MacFarlane, Nuclear data libraries from Los Alamos for fusion neutronics calculations, Trans. Am. Nucl. Soc. 36 (1984) 271.

[33] R.D. Boyd, C.P.C. Wong, and Y.S. Cha, Technical assessment of thermal-hydraulics for high heat flux fusion components, Sandia National Laboratory report SAND84-0159 (1985).

[34] W.H. Jens and P.A. Lottes, Analysis of heat transfer, burnout, pressure drop and density data for high pressure water, U.S. Atomic Energy Commission report ANL-4627 (1951).

[35] Steam/its generation and use, Babcock & Wilcox Co. (1978).

[36] G.J. DeSalvo and J.A. Swanson, ANSYS User's Manual, Swanson Analysis Systems, Inc. (1979).

[37] D.L. Smith, G.D. Morgan, M.A. Abdou, C.C. Baker, J.D. Gordon, et al., Blanket comparison and selection study – Final Report, Argonne National Laboratory report ANL/FPP-84-1 (1984).

[38] K.Y. Wong, T.A. Khan, F. Guglielmi, et al., Canadian tritium experience, Ontario Hydro report (1984).

[39] D.K. Sze, TITAN tritium, Fusion Engrg. Des. 23 (1993), in this issue.

[40] M. Abdou, C. Baker, J. Brooks, et al., A Demonstration Tokamak Power Plant Study (DEMO), Argonne National Laboratory report ANL/FPP/82-1 (1982).

[41] P.J. Burns, TACO2D – a finite element heat transfer code, Lawrence Livermore National Laboratory report UCID-17980, Rev. 2 (1982).

[42] J.P. Holdren et al., Summary of the Report of the Senior Committee on Environmental, Safety and Economic Aspects of Magnetic Fusion Energy, Lawrence Livermore National Laboratory report UCRL-53766 (1987); also J.P. Holdren et al., Exploring the competitive potential of magnetic fusion energy: the interaction of economics with safety and environmental characteristics, Fusion Technol. 13 (1988) 7.

[43] S.J. Piet, Approaches to achieving inherently safe fusion power plants, Fusion Technol. 10 (1986); also: Inherent/passive safety for fusion, Proc. 7th ANS Topical Meeting on Tech. of Fusion Energy, Reno, NV (1986).

[44] F.M. Mann, Transmutation of alloys in MFE facilities as calculated by REAC (a computer code for activation and transmutation calculations), Hanford Engineering and Development Laboratory report HEDL-TME 81-37 (1982).

[45] Standards for protection against radiation, U.S. Nuclear Regulatory Commission, Code of Federal Regulations, Title 10, Part 0 to 199 (1986).

[46] S. Fetter, E.T. Cheng, and F.M. Mann, Long-term radioactivity in fusion reactors, Fusion Engrg. Des. 6 (1988) 123.

[47] G. Malesani and G. Rostagni, The RFX experiment, Proc. 14th Symp. Fusion Technology, Avignon (1986) 173.